



Mechanical Particle-Size Reduction Techniques

4

Javier O. Morales, Alan B. Watts, and Jason T. McConville

Abstract

With the increasing number of new drug candidates, the number of those that have poor aqueous solubility is also on the rise. To overcome this limitation, a common formulation approach has been to decrease drug particle size. This strategy results in increased surface area, the potential to increase saturation solubility, and decreased diffusional distance, all of which lead to an increase in the extent and the rate of dissolution. Mechanical techniques to decrease the particle size of solids are generally classified in three categories: dry milling, wet milling, and high-pressure homogenization. In order to produce particles in the submicron (nano) range and further increase solubility, techniques such as wet-media milling, piston-gap

homogenization, and microfluidization have been developed. More recently, combination technologies of both top-down and bottom-up approaches have gained much interest. All these different strategies are reviewed and discussed in this updated chapter. This current third edition chapter is a revision and update of the original authors' work from the first and second editions.

Keywords

Dry milling · Wet milling · Nanocrystal · High-pressure homogenization · Cryomilling · Nanoedge technology

J. O. Morales (✉)

Department of Pharmaceutical Science and Technology,
School of Chemical and Pharmaceutical Sciences,
University of Chile, Santiago, Chile

Advanced Center for Chronic Diseases (ACCDiS),
Santiago, Chile

Center of New Drugs for Hypertension (CENDHY),
Santiago, Chile

e-mail: jomorales@ciq.uchile.cl

A. B. Watts

Catalent Pharma Solutions, Somerset, NJ, USA

J. T. McConville

Department of Pharmaceutical Sciences, University of
New Mexico, Albuquerque, NM, USA

4.1 Introduction

The percentage of newly discovered drugs that have poor water solubility has been trending upward, and products with market approval in the pharmaceutical industry include approximately 40% poorly water-soluble compounds and nearly 90% of new drugs in the discovery pipeline (Kalepu and Nekkanti 2015; Lipinski 2000). Of the total of drugs in the pipeline, up to 60% are derived directly from synthesis (Gribbon and Andreas 2005; Lipinski et al. 1997). Aside from the most notable limitation, i.e., poor bioavailability, these compounds are hard to formulate due to a number of other factors such as fed versus fasted bioavailability variation, lack of

dose–response proportionality, suboptimal dosing, use of problematic excipients (such as cosolvents), use of extreme basic or acid conditions to optimize solubilization, uncontrollable precipitation after dosing, and inconvenience of the dosage form (Merisko-Liversidge and Liversidge 2008). Over the years, a number of different strategies have been developed in order to overcome these limitations. Some of these efforts include creating salts, prodrugs, and screening for more soluble analogs. However, these efforts have achieved limited success, and the need of novel strategies has been the driving force for the development of technologies to improve the bioavailability-related outcomes of poorly water-soluble drug molecules. Extensive research into the development of novel techniques to engineer micron-scale particles to the nanoscale range has translated into various proprietary technologies. Technologies that have been commercialized to decrease drug particle size into the nanosize range for marketed products include the NanoCrystal® technology developed by Elan Drug Technologies (now Alkermes), which is a high-energy media milling technique (Elan Drug Technologies—Commercialized Products 2010), and the Insoluble Drug Delivery Microparticle technology (IDD-P®) by SkyePharma (SkyePharma—Insoluble Drug Delivery Platform 2010). Other marketed products have been developed using media milling and high-pressure homogenization (Fontana et al. 2018).

Nonspecific formulation approaches are applicable to almost any drug molecule (apart from a few exceptions). Micronization has been for many years the most widely used nonspecific approach, which consists of converting relatively coarse drug particles to micrometer-sized particles with a mean diameter in the range of approximately 2–5 μm and a corresponding size distribution approximately between 0.1 and 20 μm (Muller et al. 2006). Nonetheless, many novel drugs are so poorly soluble that a further decrease in particle size is often required in order to obtain acceptable solubility. Particle-size reduction techniques increase the surface area, leading to an increase in the solubility by

mechanisms that will be explained in this chapter. An increase in solubility is one of the reasons for reducing the particle size of pharmaceutical powders; and particle-size reduction is applied in several fields within the pharmaceutical sciences, such as pulmonary drug delivery, solid oral dosages, and powder handling.

It is known in the literature that pulmonary drug delivery by dry powder inhalation is an administration route where particle-size reduction is required to reach the target region of the lung. The aerodynamic diameter of a particle should be in the critical range of 0.5–5 μm (Clark and Shire 2000) to reach appropriate regions of the deep lung for maximum absorption (Hassan and Lau 2010). This size range can be achieved by many of the various milling technologies (Chow et al. 2007).

Additionally, many pharmaceutical processes involving powders can be improved by homogenizing the particle size of the drug and excipients. Solids produced by uncontrolled crystallization or precipitation processes can have a broad size distribution that can result in poor flow properties or tendency to segregate. Blending, compressibility, flow/suspension behavior, and compaction performance can all vary with a heterogeneous particle-size distribution (Fisher 2006). Furthermore, the particle-size distribution of very potent drugs, requiring low content in the final dosage form, is usually homogenized before blending with excipients in order to provide adequate content uniformity (Clement and Purutyan 2002; Rohrs et al. 2006).

Bulk active pharmaceutical ingredient (API) production may often be limited by specified particle-size profiles to meet the need of formulation and pharmaceutical processes. The ability to control the particle size during early stage API development and to predict the operating conditions that will produce that particle size reproducibly at commercial scale is very important. Furthermore, a final milling process may be required in order to narrow the particle-size distribution across batches so that better flow and handling properties are produced, or match an API particle size more closely with the combined

excipient(s) particle size to minimize the potential for segregation during blending (Fisher 2006).

4.2 Rationale Behind the Reduction of Particle Size

As stated earlier, a decrease in particle size to the few micron range and down to the nanosize range can potentially increase the extent and rate of solubility of drugs. This is of high relevance for poorly water-soluble compounds since this feature is their main limitation. Decreasing the particle size to the micron range substantially increases the exposed surface area of a given amount of powder. The micronized powder can then be further engineered, and its particle size further decreased to the nanosize range, when the surface area increases sharply as can be depicted in Fig. 4.1 (Merisko-Liversidge and Liversidge 2008).

This has a direct effect on the dissolution rate according to the Noyes–Whitney equation as depicted in (4.1) (Noyes and Whitney 1897):

$$\frac{dm}{dt} = \frac{DA_s(C_s - C)}{h_H} = kA_s(C_s - C), \quad (4.1)$$

Where m is the undissolved solid particle mass of solids, t the time, h_H the diffusion boundary layer thickness, D the diffusion coefficient, k the intrinsic dissolution constant, A_s the surface area

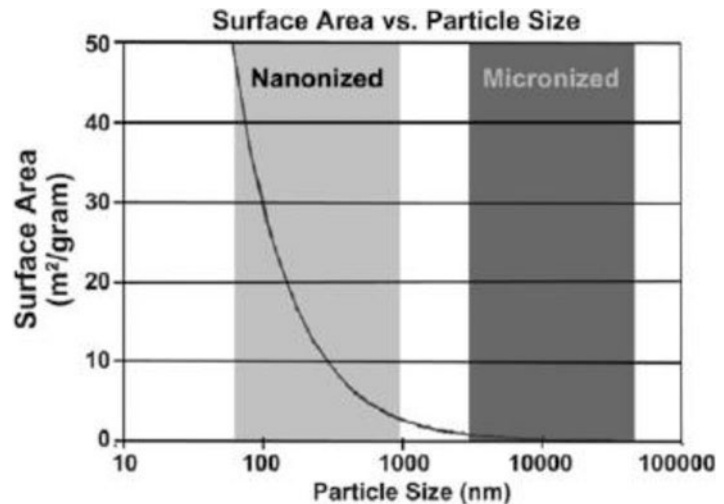
of the dissolving solid, C the concentration of solute in solution, and C_s the saturation solubility. This translates into three main factors that can affect the dissolution rate: surface area, saturation solubility, and diffusional distance.

The Kelvin equation describes the increase in vapor pressure as a function of the curvature of liquid droplets, which ultimately translates into an increase in the saturation solubility as seen in (4.2) (Simonelli et al. 1970):

$$n \frac{P_r}{P_\infty} = \frac{2\gamma V_m}{rRT}, \quad (4.2)$$

Where P_r is the vapor/dissolution pressure with particle radius r ; P_∞ is the vapor/dissolution pressure with infinite particle size; γ is the interfacial tension; V_m is the molar volume; R is the gas constant; T is the absolute temperature; and r is the particle radius. When the particles are suspended in a saturated solution, it can be assumed that the P_r/P_∞ ratio can be approximated to the ratio of the respective activities of small and large particles. Furthermore, if the activity coefficients of both particles are equal, the activities can be replaced by their respective solubilities. Similar to the sharp increase in surface area observed for very small particle size, reducing the particle size below the size threshold of 1–2 μm leads to a distinct increase in the dissolution pressure, thus shifting the solubility equilibrium toward an increased saturation

Fig. 4.1 The plot demonstrates the increase in surface area obtained when solids are fractured from the micrometer-size range to the nanometer-size range (Merisko-Liversidge and Liversidge 2008)



solubility. This is expressed in the Ostwald–Freundlich (4.3) (Simonelli et al. 1970):

$$\ln \frac{C_{s,r}}{C_{s,\infty}} = \frac{2\gamma V_m}{rRT}, \quad (4.3)$$

Where $C_{s,r}$ and $C_{s,\infty}$ are the solubilities of a particle of radius r and of a very large particle (or an approximately flat surface with very low dissolution pressure), respectively.

An additional factor that enhances the dissolution velocity is a decrease in the diffusion distance at very small particle size as is described in the Prandtl boundary layer (4.4) (Bisrat and Nyström 1988), which translates into an increase in the concentration gradient ($C_s - C$):

$$h_H = k \left(\frac{L^{1/2}}{V^{1/2}} \right), \quad (4.4)$$

Where h_H is the diffusion boundary layer thickness, L is the length of the surface in the direction of flow, k denotes a constant, and v is the relative velocity of the flowing liquid against

the flat surface. In addition to the above statement, this can be extracted from the Prandtl equation, where individual particles will have a very small surface exposed in the direction of the flow, which will ultimately decrease the distance that the molecules need to diffuse going into the bulk of the solution.

The equations presented here are clear evidence that reducing the particle size results in larger surface area, elevated saturation solubility, a decrease in the diffusional distance for drug molecules, and therefore a faster rate of dissolution as summarized in Fig. 4.2.

Additionally, high-energy processes, such as those used in top-down methods for particle-size reduction, can be associated with transitions from the crystalline state to an amorphous state (Muller et al. 2003). Transformations to the amorphous state or to different polymorphs have also been observed during high-energy input processes, such as tableting (Chan and Doelker 1985; Koivisto et al. 2006; Zhang et al. 2004). High-

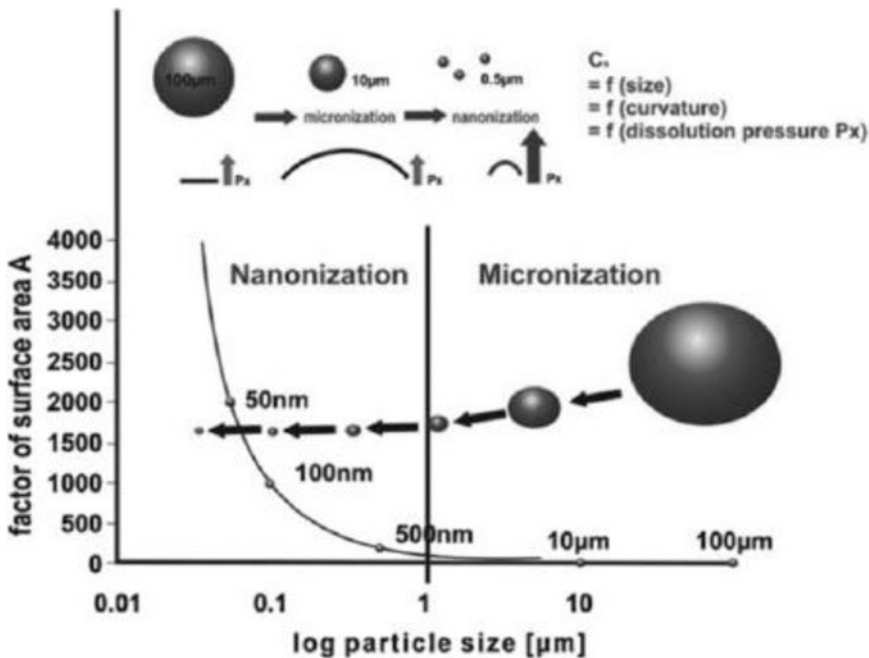


Fig. 4.2 Changes in properties when decreasing the particle size from the micro- to the nanorange. *Top insert:* Decreasing the particle size increases the particle size and therefore increases the dissolution pressure, increasing the

saturation solubility. *Bottom figure:* Decreasing the particle size results in an increase in surface area, being pronounced below 1 µm and very pronounced below 100 nm (Shegokar and Müller 2010)

pressure homogenization is a commonly used top-down process to obtain micro- and nanoparticles and is one such high-energy process; the drug particles are exposed to a power density of up to 10^{13} W/m³ (Muller et al. 2003). This high energy breaks down the drug particles into microparticles and into nanoparticles, and can also induce the change to an increased amorphous fraction or to completely amorphous particles (Böhm et al. 1998; Dong and Feng 2007; Jacobs et al. 2000; Ward and Schultz 1995) (Fig. 4.3). It is known in the literature that the amorphous state yields a higher saturation solubility than that exhibited by the crystalline structure of the same drug (Agrawal et al. 2004; Hancock and Parks 2000; Murdande et al. 2010). Considering the solubility enhancement inherent in the decrease in particle size discussed earlier, amorphous nanoparticles may exhibit very high saturation solubility compared to the crystalline form prior to processing.

Furthermore, decreasing the particle size of drugs can increase the stability of formulations. An example of this can be found in nanosuspension formulations of paclitaxel. Paclitaxel is a highly water-sensitive molecule that when dissolved in water degrades to an extent of 80% within 25 minutes (Liversidge and Wei 2003). It has been found that the production of an aqueous nanosuspension, with the use of surface stabilizers, can increase the stability over a period of 4 years when stored at 4 °C, i.e., more than 99% of the drug remains intact after recovery (Troester 2004).

The following sections will discuss the theory and applications of various top-down techniques used in the field for decreasing the particle size of

drugs. These techniques can be divided into two main groups: milling and high-pressure homogenization.

4.3 Milling

Milling processes can be divided into dry or wet milling depending on the media in which the powders are milled, namely gas or liquid. In both cases, particle-size reduction occurs by collision of particles with the surfaces of the equipment as well as with each other. The collision events involve compression, impact and attrition, and cutting or shear as the main mechanisms for particle-size reduction (Clement and Purutyan 2002; Friedrich 2001; Spencer and Dalder 1997). Additionally, the wet-milling process also involves liquid shear forces or cavitation, ultimately resulting in particle-size reduction (Rabinow 2004; Sharma et al. 2009) (Table 4.1).

The density of solids in the mill is an important parameter directly affecting breakage mechanisms. Density has a direct relationship with the number of particle–particle or particle–wall collisions as well as the force of the collisions (Bentham et al. 2004). Feed rate to the mill and mill residence time also directly affect the solid particle concentration of solids in the mill. Thus, an understanding of the particle density in the mill is crucial since it can impact the milling rate and efficiency, both of which are important for scale-up purposes. For example, research in Thailand demonstrated that by increasing concentrations from 30 to 55% solids (by volume), the mill net power increased with

Fig. 4.3 Schematic representation of a crystalline surface before and after mechanical comminution. After milling, the surface that has been exposed to collisions is disrupted and may exhibit amorphous domains (Ward and Schultz 1995)

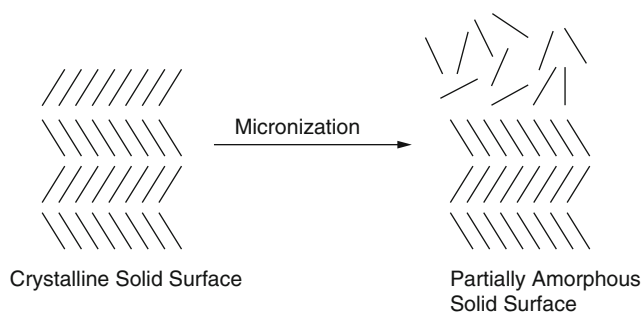


Table 4.1 Comparison of dry and wet milling

	Dry milling	Wet milling
Medium	Air	Liquid
Medium property	Compressible	Noncompressible
Force/energy transfer	Particle–particle collision Particle–equipment collision	Particle–particle collision Particle–equipment collision, liquid shear forces, and cavitation
Inertial dampening of forces	Weak to none	Strong

increased powder filling, and then decreased after an optimum value was achieved (Tangsathitkulchai 2003).

Due to the nature of the milling process, the milled powders produced always exhibit a range of particle sizes or a characteristic particle-size distribution. In many cases, this range of particle sizes obeys a log normal distribution; however, some processed powders can exhibit multimodal distributions. Therefore, when the goal of milling is to meet a specific unimodal particle-size range, a classification step may be needed. Several mills available in the market can perform both operations (particle-size reduction and classification) in sequential steps in one instrument (Fisher 2006; Steckel et al. 2006). The influence of the feed particle size can be diminished when the milling equipment includes internal classification or if a separate classifier is part of the process line. Additionally, the solid particle feed rate and the intrinsic density of the particles play a fundamental role in the intensity of the interparticle collisions; therefore, controlling both factors will determine particle-size distributions and reproducibility in a given milling process.

Another parameter that is relevant to consider is the target and achieved surface area during the milling process. As stated earlier, decreasing the particle size of a solid increases the overall surface area exposed, affecting dissolution performance. Even so, since the value of surface area is a scalar quantity representing the totality of the processed powder, it does not provide a sense of the range of particle sizes. Therefore, in the development of controlling parameters during the milling process, determining the particle-size distribution is crucial for the performance of the engineered powder. It is normally recommended to control for particle-size distribution alone,

instead of surface area together with distribution since they are so closely related (Clement and Purutyan 2002).

Even though understanding the equipment capabilities and the mechanism of particle-size reduction is critical in selecting the appropriate mill, specific powder properties such as hardness, friability, and fracture toughness will affect the milling performance in both dry- and wet-milling equipment alike (Chaumeil 1998; Kesisoglou et al. 2007). It is common for milling equipment to be described in terms of the particle sizes that can be achieved, and for this purpose, the Mohs scale is used as an indicator of particle hardness and for estimating the mill performance (Clement and Purutyan 2002). This scale ranges from a hardness of 1 for soft materials to a value of 10 for the hardest material (diamond). Additionally, particle morphology or aspect ratio can affect milling results in various ways. For example, it has been shown that β -succinic acid crystals with plate-like morphology are more prone to crystallinity loss on milling compared to those with needle-like morphology (Chikhalia et al. 2006). Therefore, a thorough understanding of the properties of the solid, together with the specific mechanism of particle-size reduction of the milling equipment, is of high importance.

One of the most relevant limitations of milling is to actually control and narrow the particle-size distribution; this is normally optimized by controlling for several parameters in the process. In general, capital costs for installation are high, and the operation of the equipment can be labor intensive (Fisher 2006). Additionally, while milling can allow for a reduction of the aspect ratio, it is not normally able to control the particle shape. Furthermore, some active pharmaceutical ingredients may not be able to be processed

through milling due to either compaction sensitivity (losing crystallinity), temperature sensitivity (melting or changing to a different polymorph), or changing hydration state (Peltonen and Hirvonen 2010; Shoyele and Cawthorne 2006). Therefore, depending on the API characteristics, milling may not always be the best choice to reduce the particle size of powders.

It is relevant to note that wet mills such as rotor–stator media mills (Netzsch Pumps North America, LLC, Exton, PA) or dry mills such as jet mills (Retsch GmbH, Haan, Germany) are limited in the production of solid particles in the nanometer scale (Muller et al. 2006). For example, it has been found that usual range of particles in a jet mill can be from 0.1 to 20 μm , with only a 10% in the submicron range (Muller et al. 1995). On the other hand, nanoparticles have been obtained by using ball media mills for extended periods of time (Liversidge et al. 1992; Merisko-Liversidge et al. 1996; Merisko-Liversidge et al. 2003). The following sections focus on several dry- and wet-milling techniques, describing important parameters, particle-size ranges, and applications of each technique.

4.3.1 Dry Milling

As mentioned above, particle-size reduction in dry mills occurs by pressure, friction, attrition, impact, or shearing by particle–particle or particle–equipment interactions. Even though a variety of mills are available for decreasing the particle size, some common issues can be identified. In general, issues related to the dry-milling process may include powder accumulation that can impact performance and

electrostatic agglomeration of milled particles that may hinder the API dispersion during formulation (de Villiers 1995; de Villiers and Tiedt 1996). Furthermore, the moving parts of some dry mills can generate considerable frictional heat. For example, during powder processing in a pin mill, the internal temperatures can reach 40–60 $^{\circ}\text{C}$ (Fisher 2006), which can impose a limitation to certain pharmaceuticals. For these types of powders, cryomilling could be an option and is discussed in further detail later in this chapter.

In the scale-up process, the flow properties of the dry powder being deposited into the mill could affect uniformity of delivery. Furthermore, if the milled or partially milled product is very cohesive (either inherently or due to electrostatic charge), it could accumulate, and the overall process yield could be reduced. Removing the product periodically from low flow areas (cyclones, pipe elbows, and bends) can increase the cost and extend the processing time. If material were to accumulate in the mill, especially in places that could block the exit of the mill, this could result in equipment overheating and eventual failure.

Manufacturers of mills normally report the correlation between particle hardness (on the Mohs scale) and the extent of size reduction that could be achieved in a particular mill. A general lower limit can be described for mills, depending on the mechanism of action and the amount of energy that it can provide for grinding. The following sections describe the dry-milling equipment used for decreasing the particle size of pharmaceutical powders (Clement and Purutyán 2002; Fisher 2006; Friedrich 2001) (Table 4.2). While most dry-milling techniques can render particles in micrometer-size range, recent investigations have developed formulations that

Table 4.2 Types of dry-milling equipment categorized by average particle size achievable and hardness of materials it can process

Mill type	Typical minimum particle size achieved (μm)	Maximum hardness (on the Mohs scale)
Cutting mill	150	Soft
Pin/cage mill	10–50	Soft, up to 3
Hammer mill	10–75	Intermediate, up to 6
Jet mill	2	Soft, up to 3
Fluidized bed jet mill	2	Hard, up to 10
Ball mill	<1	Hard, up to 8

can achieve drug nanoparticles of lamotrigine by co-milling with polyvinyl alcohol (Ambrus et al. 2020; Gieszinger et al. 2018). Using a quality by design (QbD) approach, and after definition of the design space, selected conditions yielded mean particle sizes as low as 97 nm (Gieszinger et al. 2018).

Fluidized Bed Jet Milling

The primary mechanism of particle-size reduction in the impinging jet or fluidized bed jet mill is particle–particle collisions. When the media to be milled is fed to the chamber, it is exposed to impinging high-velocity gas jets that allow for the collisions (Fig. 4.4). This type of milling equipment can process hard materials (Mohs scale hardness of up to 10), which is a prominent advantage compared to other air jet mills, such as spiral mills (Mohs scale hardness of up to 3.5) (Clement and Purutyan 2002).

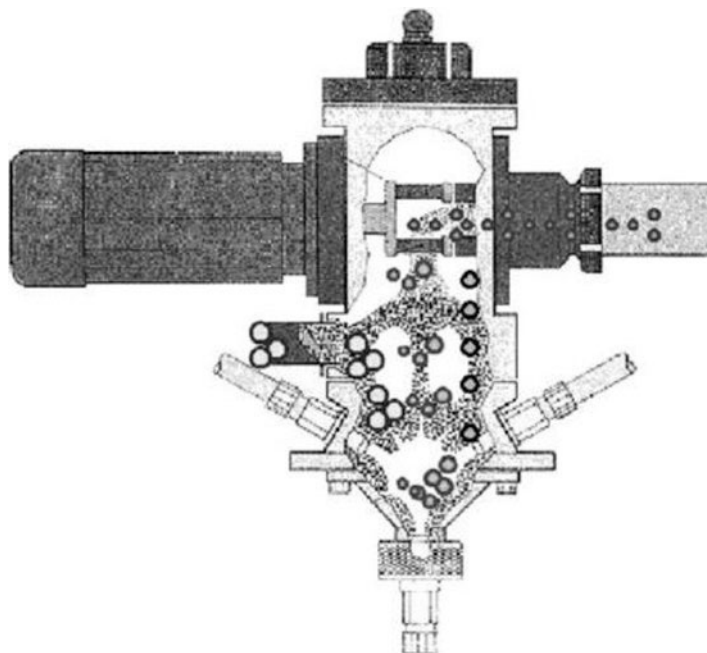
Additionally, impinging jet mills feature a separate classifier, e.g., rotating wheel, preventing unmilled solids from exiting the milling chamber until particles have reached a certain particle-size threshold (Fig. 4.4.). In the case of a rotating wheel classifier, the particle size depends on the rotation speed of the wheel and the velocity of the

gas exiting the mill (Godet-Morand et al. 2002; de Vegt et al. 2009). Varying the classifier speed is the normal technique used to control the particle-size distribution of the milled material; however, parameters such as grinding gas pressure and total gas flow rate can be modified to achieve the desired particle-size distribution and processing times. Changing nozzle diameter is the most common approach for control of these variables. It is important to note that when the parameters described here are fixed, the solid particle feed rate does not normally affect the particle-size distribution, but it does affect the residence time and processing times.

Results will vary depending on the conditions used in the equipment and the properties of the solid (Rasenack and Müller 2004). However, for typical working pressures between 3 and 10 bar, particle sizes are usually tightly distributed due to the classifier and normally range between 1 and 10 μm . Typical surface areas achieved range from 2 to 5 m^2/g and are strictly dependent on the API hardness and friability (Fisher 2006).

One of the main limitations of this type of mill is the potential for buildup of compressed product in the mill or classifier due to the particle–wall

Fig. 4.4 Scheme of a fluidized bed air jet mill (Godet-Morand et al. 2002)



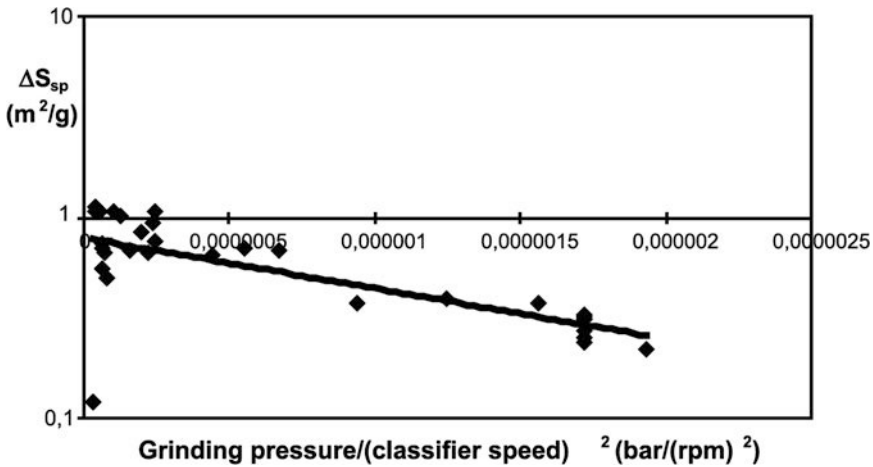


Fig. 4.5 Specific surface created as a function of the factor P/N^2 for the fluidized air jet mill. (From Nakach et al. 2004)

and particle–classifier collisions. Accumulation of product in either of these compartments will change the geometry of the mill and will alter the performance and reproducibility of the equipment. In general, buildup at the exit of the mill or in the classifier will increase the particle size over time owing to a reduced performance of the classification system. The material accumulated in the mill can become compressed or discolored or may change into an amorphous form, all of which will affect the product quality if it enters the milled batch stream. Even if intermittent cleaning is introduced in the process to avoid these problems, the impact in the overall productivity could be important.

Nakach et al. (2004) studied the effect of the air pressure at the grinding nozzles, the solid particle feed rate, and the speed of rotation of the turbo selector. In their studies, they found a dependency of the specific surface of the product with the air pressure (P) and the speed of rotation of the classifier (N) (Nakach et al. 2004). The equation below indicates the relationship between air pressure and the classifier rotational speed, with the forces present in a dry mill.

$$\frac{P}{N^2} \propto \frac{\text{dragforce}}{\text{centrifugalforce}}. \quad (4.5)$$

It was found that 1–10 kg/h solid particle feed rate had little influence on the specific surface of the product (Fig. 4.5). That particle size is mostly controlled by the classifier. Furthermore, by

recycling particles back into the mill, there is an increase in the mill holdup. The online sizing system evidenced that D_{50} and D_{90} varied considerably during operation, but D_{10} was more stable (Nakach et al. 2004).

Spiral Jet “Pancake” Mill

Spiral jet or pancake mills have jets of air tangentially located around the center of the equipment in order to create a vortex of air. Particle-size reduction is a result of particle–particle and particle–wall collisions upon feeding of solids into the air stream (Fig. 4.6). Normally, gas velocities are such that a sonic flow is achieved, and only particles that reach a predetermined particle size will be able to leave the vortex through the exit. This internal orientation is advantageous due to the classification that naturally occurs in the system. Due to centrifugal forces, larger particles tend to remain near the perimeter of the milling chamber until the particle size is reduced, and they are light enough to travel to the center of the mill due to centripetal forces.

Particle-size reduction will depend on two main variables, namely the equipment and the solid to be milled. Geometric parameters of the equipment such as shape and diameter of the grinding chamber and shape/type, number, and angle of grinding nozzles will determine the performance of the milling process. Additionally,

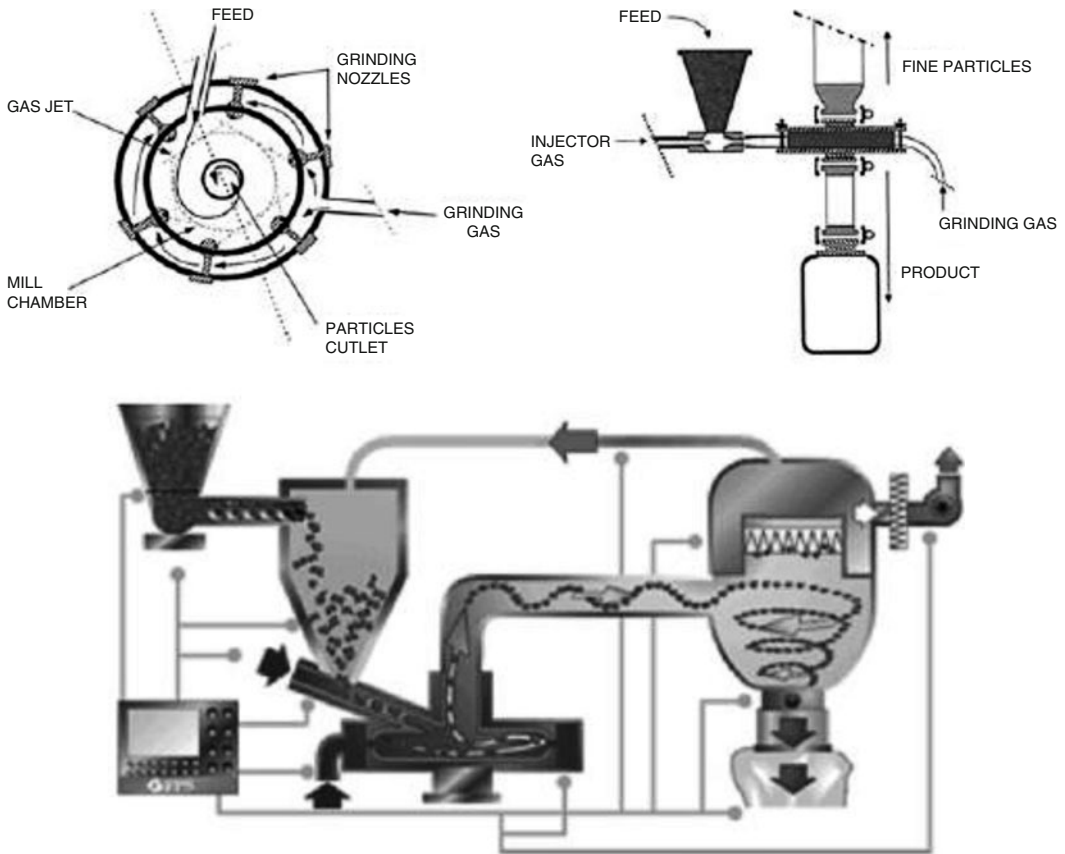


Fig. 4.6 Above: scheme of a spiral jet “pancake” mill (Midoux et al. 1999). Below: scheme of a spiral jet mill with an additional classifier online (New Food Pharma Systems Spiral Jet Mill: Introduction 2010)

operating variables such as grinding jet air pressure, total gas flow rate, and solid particle feed rate play a role in the final particle-size distribution achieved (Friedrich 2001; Hoyer et al. 2008; Midoux et al. 1999; Schlocker et al. 2006).

Geometry Dependence

Midoux et al. (1999) have described the relationship between the volumetric flow rate V_n , the solid feed rate Q , and the diameter of the mill chamber D as follows:

$$V \propto D^2. \quad (4.6)$$

Moreover, the volumetric flow rate and the feed rate can be correlated as (Ito 1987):

$$Q \propto V_n^{1.4 \pm 0.1}. \quad (4.7)$$

Finally, by combining the above two relationships, a third relationship can be defined in terms of the solid particle feed rate and the mill chamber diameter:

$$Q \propto D^{2.8 \pm 0.2}. \quad (4.8)$$

According to a survey using the manufacturer’s product information, the above-derived relationship obtained is in accordance with what had been described before, namely Q is proportional to $D^{2.3 \pm 0.3}$, as well as to Smit’s work on waxes describing a Q proportional to $D^{2.5 \pm 0.2}$ (Smit 1986). Furthermore, the exponent seems to depend on the properties of the material being ground (Midoux et al. 1999).

Nozzle Dependence

The most common nozzle geometry is the abrupt type, providing sonic velocity at the inlet with an exit pressure of about 50% of the initial fluid pressure (Fig. 4.7). A suction that entraps particles from the mill is created after the final expansion occurs beyond the nozzle inlet. This phenomenon circulates the gas and induces particle–particle collisions. In the Laval-shaped nozzle, air expansion occurs at the divergent section. This leads to supersonic velocities, increasing the air jet action and the velocity of the circulating gas, therefore producing greater particle–particle collisions and thus increasing the production rate and reducing the average particle size (Midoux et al. 1999).

Additionally, regardless of the type of nozzle, the number of nozzles is an important factor to consider in the performance of a jet mill. The influence of three different configurations, 3, 6, and 12 nozzles, while maintaining the total section of the nozzles and varying the solid's feed rates, has been studied (Skelton et al. 1980). It was found that a greater number of nozzles created a more regular pitch circle; furthermore, thinner jet nozzles led to minor perturbations of the spiral flow in the chamber. Accordingly, the design including 12 nozzles exhibited the best grinding ratio. Moreover, increasing the feed rates was also found to improve the grinding ratio.

The angle at which the nozzles are oriented toward the inner chamber of mill can be modulated, and their optimal values have been reported in the literature. If the angle is measured

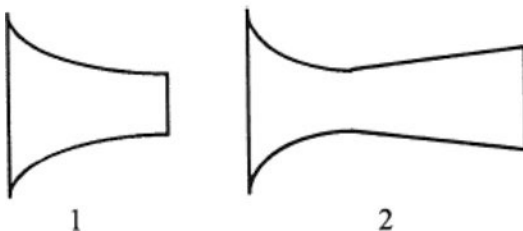


Fig. 4.7 The (1) abrupt nozzle and (2) Laval-shaped nozzle. In the scheme, the flow is from *left to right* (Albus 1964)

with respect to the tangent, Smit's optimum value was equal to 58° (Smit 1986) and Skelton's was between 52° and 60° (Skelton et al. 1980). Nonetheless, other operating angles ranging from 63° to 67° have been described in the literature (Midoux et al. 1999).

Working Conditions

In addition to the geometry of the chamber and the nozzles, operating variables can be controlled to obtain different outcomes. One of these variables is grinding pressure, which controls the gas mass flow rate input. As described by Midoux et al. (1999), if one assumes that the nozzles are isentropic, the initial grinding pressure P and the pressure at the nozzle throat P_t are related according to (4.9):

$$\frac{P}{P_t} = \left(1 + \frac{k-1}{2} M_t^2\right)^{\frac{k}{k-1}} \quad (4.9)$$

Where M_t is the Mach number at the throat, and k is the ratio of specific heats of the gas. With this, a critical grinding pressure P_c can be defined as follows in (4.10):

$$\frac{P_c}{P_t} = \left(\frac{k+1}{2}\right)^{\frac{k}{k-1}} \quad (4.10)$$

This critical grinding pressure is equivalent to the minimum pressure that yields a sonic flow at the nozzle inlet. Above this value, the gas mass flow rate M_g can be expressed by (4.11):

$$M_g = PA \sqrt{\frac{M_w k}{RT} \left(\frac{2}{k+1}\right)^{\frac{k+1}{k-1}}} \quad (4.11)$$

As can be derived from the (4.11), M_g is directly proportional to the grinding pressure P , the throat section A , and the molecular weight M_w of the fluid employed for grinding. The gas kinetic energy (E_k) can be defined by (4.12):

$$E_k = \frac{1}{2} M_g v_g^2 \quad (4.12)$$

The concept of specific energy consumption (E_{sp}) has been used in the literature (Kaiser and Nied 1980; Schurr and Zhao 1994; Stairmand

1975) to correlate solid's feed rate and grinding pressure, which is directly correlated to the gas kinetic energy (defined above). According to Schurr and Zhao, this is calculated by (4.13) (Schurr and Zhao 1994):

$$E_{sp} = \frac{\dot{E}_k}{Q}. \quad (4.13)$$

With this value, different mills and different working conditions can be compared on the same system. In a spiral jet mill, the specific surface area (SSA) of the product is related to E_{sp} by a power function as follows in (4.14):

$$SSA \propto E_{sp}^x. \quad (4.14)$$

In their studies, Midoux et al. (1999) corroborated that the SSA was dependent on the grinding pressure and the solid's feed rate and could compare different systems. It was found that for the same material, the specific energy required to obtain a certain grinding ratio diminishes with the mill diameter. Additionally, a different material exhibited a clear E_{sp} transition around 400 kJ/kg. Below this value, SSA was proportional to E_{sp} with an exponent of 1.1; however, above the critical value of E_{sp} , the exponent decreases sharply as can be seen in Fig. 4.8.

In general, high grinding jet pressures result in smaller particle-size distributions. The solid particle feed rate is strictly related to the solid particle concentration in the mill, and thus, higher feed rates will produce coarser particle sizes, while

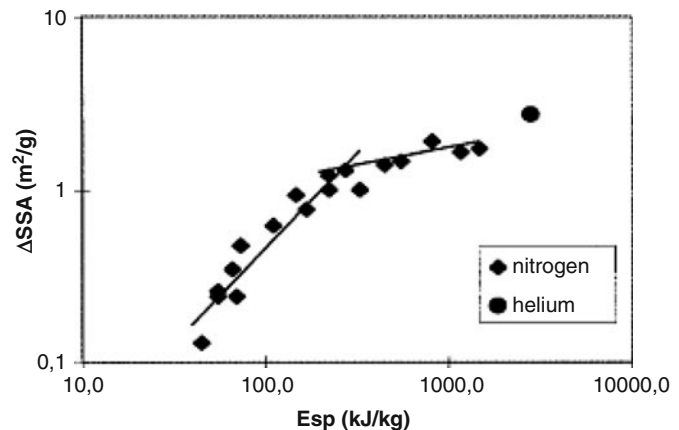
lower feed rates will result in smaller particles (Midoux et al. 1999). The literature describes that an optimal feed rate can be achieved to yield the tightest particle-size distributions at a set average particle size (Midoux et al. 1999). In general, these spiral mills are suitable for rather soft materials with a Mohs scale hardness of up to 3.5 (Chamayou and Dodds 2007). Nonetheless, they are widely used in the industry due to two main advantages: (1) there are no moving parts in the equipment, and (2) the Joule–Thomson effect produced by the expansion of the gas passing through the nozzles results in a cooling effect within the mill. This effect can help to control or suppress any local temperature increases that may be due to friction consequential of the milling process itself (Fisher 2006).

Pin Mill

A pin mill is a mechanical energy impact mill. Of all dry mills used without a particle classifier, the pin mill achieves the smallest average particle sizes (Nied 2007). In the pin mill, rotating elements in the equipment allow for particle–particle and particle–mill collisions. A limited internal classification can be achieved if appropriate elements are selected as milling tools.

The milling equipment comprises two disks fitted with overlapping pins as depicted on Fig. 4.9. The pin mill is a type of rotor–stator mill; therefore, one of the disks is the stator and the other one rotates with a high peripheral speed of up to 150 m/s. An additional modification of

Fig. 4.8 Correlation between E_{sp} versus ΔSSA



the design consists of having two counterrotating pin disks, which allow for peripheral speed of up to 250 m/s (Nied 2007). The solids are fed at a controlled rate into the center of the stator by means of a screw. They are crushed through intermeshing rings of the rotor and stator pins and the milled product leaves by centrifugal forces to the periphery to be collected or further processed.

Besides the physical properties of the solid material itself, the final average particle size of the milled product is determined mainly by rotor

tip speed, solid particle feed rate, and gas flow rate through the mill. By optimizing the process, small average particle sizes can be achieved when rotor tip speed is maximized, and both solid particle feed rate and airflow rate are minimized (Muller and Polke 1999). This is illustrated in Fig. 4.10, where it can be seen that D_{90} decreases with increasing tip speed but increases when the solid particle feed rate is increased. The rotor tip speed is an adequate way to achieve comparable results for scaling-up purposes (Fisher 2006).

An investigation by Nakach et al. (2004) studied the effect of variables such as the tip speed (or rotation speed) and the solid particle feed rate. Additionally, the effect of the type of pin mill was studied in terms of manufacturer and whether the equipment was a single- or double-rotor pin mill (Nakach et al. 2004). As can be seen in Fig. 4.11, the SSA increases linearly with the square of the peripheral speed up to 150 m/s for the different sizes of mills studied (expressed as diameter in mm).

Further studies with a pin mill attached to a dynamic selector found that the product quality was essentially dependent on the performance of the selector (Fig. 4.12). The selector had 12 blades and rotated up to 5000 rpm. After the solid was milled in the pin mill, only fine particles are able to enter the selector due to the centrifugal force repulsing the pass of coarser particles, which are brought back to the milling chamber until a suitable particle size is achieved. This mode of

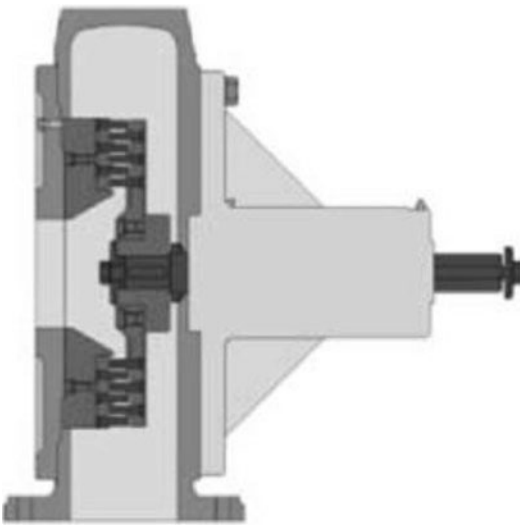


Fig. 4.9 Schematic representation of a pin mill in which the rotor and the stator are pin disks (Nied 2007)

Fig. 4.10 Influence of tip speed and solids feed rate on reducing the particle size, expressed as D_{90} in μm (Muller et al. 1999)

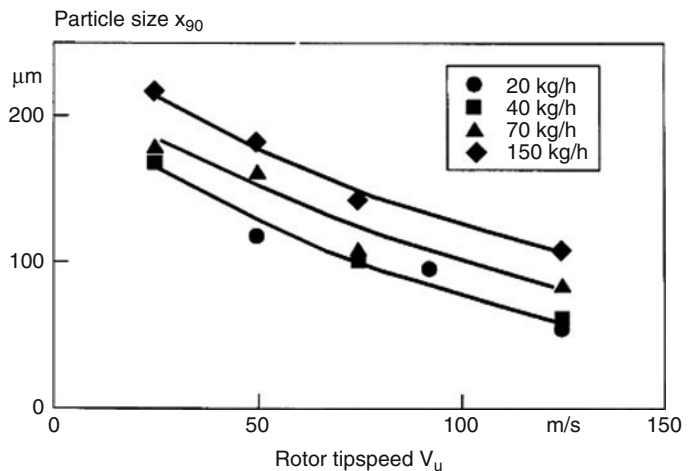


Fig. 4.11 Specific surface as a function of the square of the peripheral speed for three different sizes (expressed as diameter in mm) and types of mills (Nakach et al. 2004)

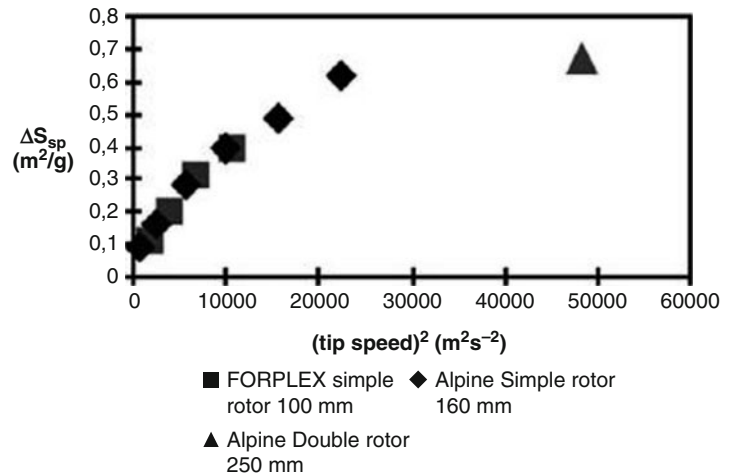
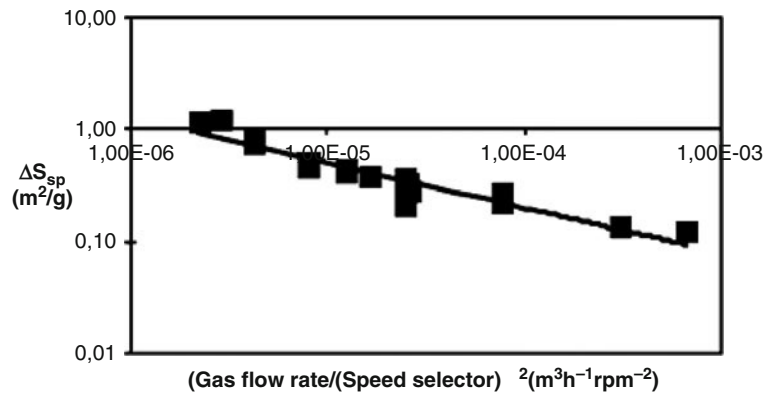


Fig. 4.12 Relation between the specific surface area and the factor P/N^2 in a pin mill with a dynamic selector (Nakach et al. 2004)



operation is similar to what has been described for fluidized air jet mills, and SSA is dependent on the air pressure P and the speed of rotation of the selector N (see (4.5)).

One of the main concerns with the use of pin mills (and any impact mill) is the generation of heat due to friction (am Ende and Rose 2006). This is of particular importance for thermally labile drugs and materials, with relatively low phase-transition temperatures (<80–100 °C). Inadequate training and subsequent poor operation of the mill can result in increasing the temperature beyond normal ranges. For example, if the feed rate is higher than the discharge rate, the mill can be “choke fed,” such that there is an accumulation of solids in the mill chamber, resulting in heat buildup. As stated above, with other types of milling equipment, due to the high

temperatures generated in the milling chamber, phase transitions may occur and amorphous material could be formed during the operation (Fisher 2006). This phenomenon has direct consequences for stability of the product and can affect the performance reproducibility from batch to batch.

Depending on the properties of the solid, the average particle sizes and the surface areas obtained in impact mills can range from 5 to 20 μm and from 1 to 2 m^2/g , respectively (Fisher 2006).

Environmental Limitations of Dry Milling

Even though the particle-size reduction mechanisms involved in the previously described mills may differ, in general, during the process of dry milling, a large amount of small size particles

Table 4.3 Means of preventing and mitigating dust explosions (Eckhoff 2003)

Prevention		Mitigation
Preventing ignition sources	Preventing explosive dust clouds	
Smoldering combustion in dust, dust flames	Inerting by N ₂ , CO ₂ , and rare gases	Partial inerting by inert gas
Other types of open flames	Intrinsic inerting	Isolation (sectioning)
Hot surfaces	Inerting by adding inert dust	Venting
Electric sparks and arcs, electrostatic discharge	Dust concentration outside explosive range	Pressure-resistant construction
Heat from mechanical impact (metal sparks and hot spots)		Automatic suppression
		Good housekeeping (dust removal and cleaning)

are produced, also known as fines, and they need to be minimized in order to prevent operator exposure and reduce the environmental impact. If recovery of the fines is needed in order to combine the fraction with the batch bulk material, a pharmaceutical grade dust collector could be used (Boundy et al. 2006).

Additionally, most milled APIs produce a potentially explosive dust (Fisher 2006; Hamelmann and Schmidt 2003). Certified laboratories perform studies of minimum ignition energy (MIE), which is the least amount of energy that is required to ignite a dust sample. For the purpose of a safe estimation, the concentration of dust used is that which will allow for the minimum energy input for ignition. An MIE lower than 20 mJ indicates that low energy sources can potentially ignite the dust sample (Stevenson 2001). For example, static electricity discharge could be one of the low-energy sources that could potentially create the explosion (Eckhoff 2003). In cases like these, a thorough and careful evaluation of the processing environment is needed in order to prevent any conditions that could yield sufficient energy to create a dust explosion. In data from Merck and Co., Inc., regarding MIE values (in mJ) for dust samples (Fisher 2006), it has been found that even though the majority of the samples do not impose a risk for explosion, 20% of the samples have an MIE of 10 mJ or less, requiring special handling conditions to prevent ignition.

There are three main strategies used for dust explosion control, namely preventing the

development of explosive mixtures (dust clouds), preventing the occurrence of ignition sources, and strategies for mitigation (Table 4.3).

A common source of ignition in the industry is the presence of hot surfaces. Contrary to what has been accepted in the past, minimum hot-surface ignition temperatures of dust clouds vary significantly when scaling up. To better estimate the value when scaling up, both the magnitude and the geometry of the hot surface in relation to the dust cloud should be considered (Eckhoff 2005).

Other common sources of ignition are the electric and electrostatic discharges. Switches, failures in electric circuits, and common discharge of static electricity are some examples of these sources. Parameters from the dust cloud that can contribute to the ignition are the particle-size/shape distributions, dust moisture content, dust concentration, and the dynamic state of the dust cloud with respect to the spark gap (Eckhoff 1994).

To prevent explosive dust clouds, an inert gas, such as nitrogen or carbon dioxide, can be mixed in the dust to a level where the dust can no longer ignite in the operating conditions. In contrast with what has been previously reported in the literature (Wilén et al. 1999), it has been found that the limiting oxygen concentration (LOC) increases with an increase in the initial pressure (in the range of 5–18 bar) (Schwenzfeuer et al. 2001). It has been reported that the LOC for ignition of dust clouds by electrostatic discharges or metal sparks was significantly higher than that determined in standard tests by using a very strong

pyrotechnical ignition source (Schwenzfeuer et al. 2001). Nonetheless, decreasing the oxygen in the process can impose the risk of suffocation on the operator. To overcome this limitation, it has been shown that adding a small volume percentage of CO₂ to the inert gas mixture can significantly reduce the critical oxygen threshold for suffocation (Eckhoff 2005).

Other operations, such as charging powders into other units, packaging solids from a milling system, or cleaning equipment after operation, can create a dust cloud that could lead to explosive conditions. Therefore, attention to housekeeping and the procedures used for these other operations also has importance (Fisher 2006).

With an overall industry increase in the manufacture of increasingly potent APIs, personnel protection has become particularly important. By decreasing the particle size and creating fines in the process, dry milling is an operation that increases the risk of exposure to personnel compared to wet milling (Stein et al. 2010). This could eventually dictate the choice of milling equipment due to the increased cost of production of dry milling and the protective equipment that personnel need to operate the mill. Wet milling in cases of a very potent API can be a more cost-effective choice.

4.3.2 Wet Milling

Wet milling, also known as slurry milling, is a particle-size reduction process in which the solid particles are suspended in a liquid medium. As such, wet milling has a number of advantages over dry milling, thermal control over the process being one of the most prominent. Due to the thermal control, heat-labile materials can be processed through this technique simply by the thermal properties of the liquid in the slurry. If additional cooling is needed, the liquid can be pre-cooled or cooled during the process to control the temperature. As stated above, this could prevent chemical decomposition, solid phase transitions, or melting of the material being milled (Merisko-Liversidge et al. 2003).

A common concern in submicron particle-size reduction techniques is the particle-size change due to dissolution of fine particles and/or growth on larger particles (Merisko-Liversidge and Liversidge 2008). The latter phenomenon, known as Ostwald ripening, can occur with any material and is accentuated when the solubility is a function highly dependent on temperature. This can be of particular relevance upon scaling up because the milling chamber surface area to batch volume ratio decreases, which ultimately influences the heat transfer in the process (Fisher 2006). Additionally, due to significant heating/cooling cycles that could occur during wet milling, an annealing effect could potentially be induced in the solids (Trasi et al. 2010).

The system of mechanical sealing of wet-milling equipment needs to be controlled due to two main issues that can arise: contamination of the batch and seal lifetime. For the sealing system to operate, a seal fluid is normally used for lubrication and cooling purposes. Therefore, there is always the potential of contamination of the batch with the seal fluid; thus, the fluid needs to be compatible with the solvent and API used in the milling process (Fisher 2006). Additionally, the sealing system should be thoroughly cleaned to extend the seal lifetime and decrease the chances of batch contamination.

The particle size achieved in a batch will normally depend on the type of wet-milling equipment that is used. However, in general particle size will be a function of the residence time of the slurry in the mill (Stenger et al. 2005). This residence time can be controlled by operating the system in either single-pass or recycling mode. In either modality, it is important to determine and control the slurry flow rate when considering the scale-up process. Furthermore, depending on the mill, it should take a predetermined number of passes to achieve a steady particle-size distribution.

In the pharmaceutical field, there are two common types of wet mills: rotor–stator and media (bead) mills. The latter is widely used due to its capacity to produce particle sizes in the nanoscale range but at the cost of longer milling times (Kipp 2004). The rotor–stator mill is widely used in the

field for emulsification and homogenization and can be used in the wet milling of APIs, achieving particle sizes in the 20–30 μm range (Atiemo-Obeng and Calabrese 2004; Lee et al. 2004).

Rotor–Stator Wet Milling

Rotor–stator milling equipment are also referred to as high-shear devices due to the shear rates generated during the rotation of the mixing element (rotor), which has a close proximity with the static element. Probe rotor–stator mills are useful for small-scale development and are normally used as batch process-type vessels. Even though data from this setup can be used as a reference for scaling-up purposes, the average particle sizes might not be comparable upon increasing the batch size. At the scale of tens of grams or more, a flow-through unit is the preferable choice, as these systems allow the slurry to pass through the high-shear patterns in the mill repeatedly, further decreasing particle size and narrowing the particle-size distribution (Nied 2007).

With toothed probe rotor–stator mills (Fig. 4.13), the mechanism of particle-size reduction is believed to occur as a combination of high shear and collision of particles with each other and the equipment walls (Atiemo-Obeng and Calabrese 2004). As a consequence, parameters that control the high shear of the equipment ultimately control the performance of the mill in terms of particle-size distribution. Tip speed (rotation rate of rotor \times rotor circumference), shear rate (tip speed/distance between rotor and stator), and shear frequency (rotation rate \times number of slots on rotor \times number of slots in

stator) are the typical design parameters that can be controlled in the development of a rotor–stator mill (Lee et al. 2004). For scaling-up purposes in equipment that has a fixed rotor–stator design to preserve rotor tip speed, scaling to a larger design results in milled particle sizes that are comparable to those obtained in small-scale batches.

As with other milling equipment, the solid particle concentration in the slurry will typically be directly related to the milling efficiency and cycle time. In general, increasing this total solid particle content will increase the milling rate. Nonetheless, there is a limit to the slurry concentration, in terms of limiting the flow of the media and potentially plugging the milling equipment (Atiemo-Obeng and Calabrese 2004).

In general, the average particle sizes obtained using a rotor–stator mill can be of a few microns, with a D_{95} normally not being larger than 40–50 μm (Fisher 2006). The hardness of the milled material dictates the cycle time when the goal is to obtain narrow particle-size distribution. A common phenomenon observed with hard, block-like materials is the potential for multimodal distributions (Lee et al. 2004). With these materials, breakage is believed to occur mainly at corners and edges, which translates into “chipping” of the hard material resulting in a high population of fines and larger particles yielding bi- or multimodal particle-size distributions (Table 4.4).

Media (Bead) Wet Milling

This type of mill operates by mechanically moving media (beads) together with the material

Fig. 4.13 Rotor–stator geometries: (a) simple Couette conical geometry (also known as colloid mill) and (b) toothed rotor–stator

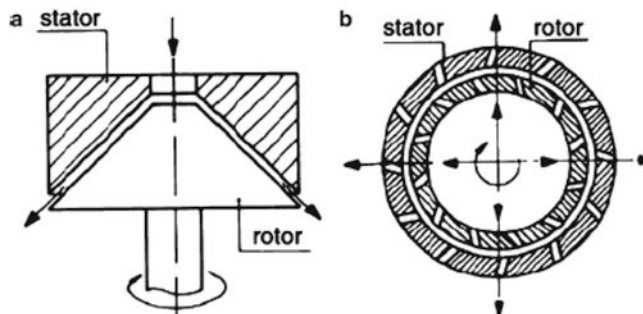


Table 4.4 Milling parameters that affect the performance of a rotor–stator wet mill (Fisher 2006)

Variable	Particle-size outcome
Rotor speed	Increasing tip speed increases milling rate and decreases average particle size. Typical range 10–50 m/s (Atiemo-Obeng and Calabrese 2004)
Rotor/stator gap	Decreasing the gap increases shear forces, increasing milling rate, thus decreasing average particle size
Rotor/stator design	The number of teeth will affect the shear forces, milling rate, and thus the average particle size achieved in steady state
Slurry density	Higher solids concentration increases milling rate but normally does not translate in a decrease in average particle size
Temperature	Higher temperature can increase product dispersion but may compromise the physical (phase transitions) or chemical (degradation) integrity of the drug
Residence time	Increasing milling time will normally decrease the average particle size

(normally the API) in a liquid. This can be done either by means of a stirrer or by agitating the container itself. The beads can be made of various materials; however, they are normally glass spheres, ceramics, metal, or plastic. The bead densities can range between 2500 and 7800 kg/m³, with sizes between 0.1 and >10 mm (Kwade and Schwedes 2007). Closed stirred media mills can be arranged either vertically or horizontally and are normally equipped with a thermal jacket for cooling purposes. According to the chamber and stirrer geometry, three types of mills can be distinguished, namely a disk stirrer, a medial mill with pin-counter-pin stirrer, and an annular gap geometry (Fig. 4.14).

The efficiency of the mill is related to a combination of many variables, such as media speed, amount of loaded media, slurry concentration, and milling time (Blecher and Schwedes 1996; Blecher et al. 1996; Kwade 2003; Schilde et al. 2010). Additionally, material properties and the overall mill design are also factors contributing to milling performance (Table 4.5).

The specific characteristics of the milling media will greatly influence the performance of the milling process. Among different geometries of the milling media, it has been found that the spherical geometry is the most effective shape (Fisher 2006). Manufacturers offer different beads with diameter ranging from 0.05 to 130 mm; however, beads 6 mm and smaller are normally used. Beads can also be obtained in various materials such as (in order of decreasing density): various grades of steel, zirconia (ZrO₂), ZrSiO₄, alumina (Al₂O₃), silica (SiO₂), annealed

glass, polytetrafluoroethylene (PTFE), and hard polystyrene derivatives (Keck and Muller 2006).

In direct comparison with a rotor–stator wet mill, media milling equipment can yield much smaller average particle sizes for the same material. Average particle sizes can range from the 1–2 μm to the nanoscale range, with adequate distribution of particle sizes when proprietary media or additives in the slurry have been used (Bruno et al. 1996; Liversidge et al. 1992). With such a pronounced particle-size decrease, surface areas in 1–2 μm size batches can be 4–5 m²/g and higher. Furthermore, nanoparticles obtained by this milling method can have a surface area of 10 m²/g or more (Fisher 2006; Muller et al. 2001).

The fundamental processes that control particle-size reduction in this type of equipment are the number of stress events and the stress intensity. In general, the average number of stress events for each particle, SN , is determined by the number of media contacts, N_C , the probability that a particle is caught and sufficiently stressed at a media contact, P_S , and the number of product particles inside the mill, N_P (Kwade 1999):

$$SN = \frac{N_C P_S}{N_P}. \quad (4.15)$$

Kwade further developed a stress model depicting the dependence of particle size, specific energy, and stress energy of the grinding media (SE_{GM}) in accordance with:

$$SE_{GM} = d_{GM}^3 \cdot \rho_{GM} \cdot v_t^2 \quad (4.16)$$

Fig. 4.14 Different stirrer and grinding chamber geometries media (beads) wet mills (Kwade 1999)

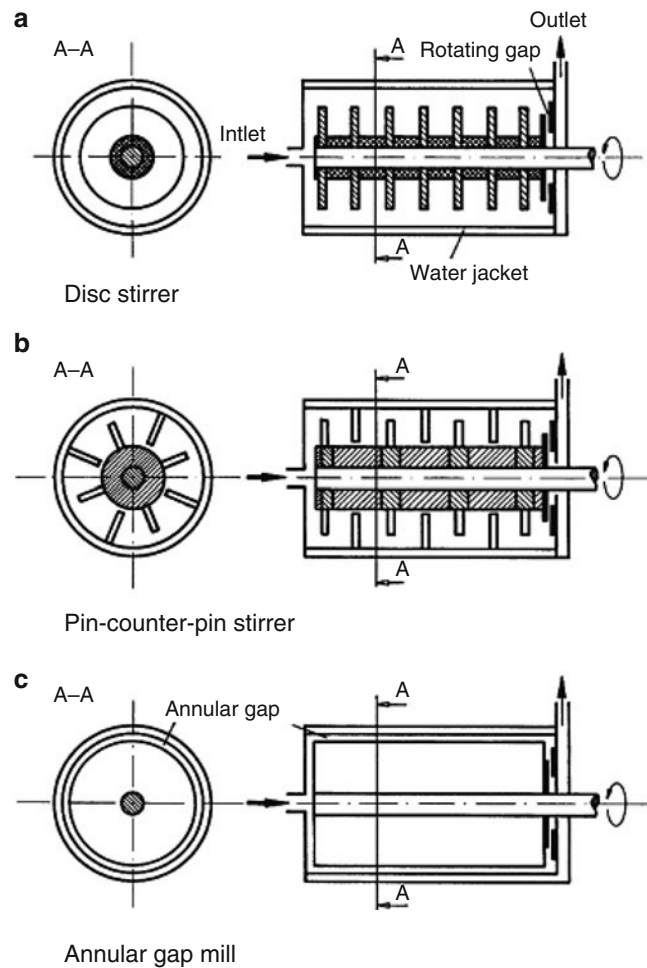


Table 4.5 Milling parameters that affect the performance of a media (bead) wet mill (Fisher 2006)

Variable	Particle-size outcome
Bead size	Decreasing the bead size normally decreases the steady-state average particle size.
Intrinsic bead density	Modifying the density of the bead can have different results, based on the material milled. In some cases, more dense beads have produced coarser product.
Bead loading	A bead charge of $\geq 50\%$ normally provides adequate milling efficiency.
Agitator speed	Increasing the linear velocity of the agitator tip increases the milling rate.
Temperature	Increasing the temperature can promote product dispersion and small average particle sizes; however, it can compromise the physical and chemical stability of the material and further dissolve very small particles.
Residence time	An increase in the residence time decreases the average particle size achieved.

Where d_{GM} is the grinding media particle size diameter, ρ_{GM} is the grinding media density, and v_t is the tip speed of the stirrer in the mill (Kwade 2003). Although this model does not consider process parameters to estimate product quality, it

was shown to work on hard inorganic materials (Kwade and Schwedes 2002). More recently, Bitterlich et al. expanded this model to the drugs (organic material) cinnarizine and fenofibrate (Bitterlich et al. 2014). While cinnarizine

exhibited a correlation between specific energy and stress energy, fenofibrate milling conditions did not show a similar correlation. The authors concluded that the employed stress energies were near the optimum region, and thus the influence of stress energy over the specific energy requirement was either very small (cinnarizine) or insignificant (fenofibrate). Furthermore, the authors highlighted the potential limitations of the stress model due to unaccounted effects such as agglomeration, ripening, and amorphization during media milling (Colombo et al. 2009).

An alternative model has been developed by Bilgili and Afolabi et al. (Afolabi et al. 2014; Bilgili and Afolabi 2012) following the work earlier developed by Eskin et al (Eskin et al. 2005a, b). In this work, the authors correlate stirrer speed, bead concentration, and drug loading on the breakage kinetics of drug particles by the adapted microhydrodynamic model for the bead–bead collisions. Several microhydrodynamic parameters derived from the model provided significant physical insight, yet the milling intensity factor (F) exhibited a strong correlation with the process time constant and was defined as follows:

$$F = \frac{c^2(2-c)}{(1-c)^3} \frac{1}{\varepsilon} \theta^{13/10} \quad (4.17)$$

Where c is the volumetric concentration of the beads, ε is the volumetric drug loading in the drug suspension, and θ is the granular temperature (Afolabi et al. 2014). This model was more recently used in reducing processing times, energy consumption, and optimizing the milling of griseofulvin and indomethacin to a sub-100 nm nanosuspension (Li et al. 2015).

As stated above, the factors determining the number of stress events and stress intensity are dependent on the design and residence time in the mill. Scaling up can therefore be complicated by the differences in relative contributions of number of stress events and stress intensity and if power per unit volume for larger mills decreases (Bell 2005). Nonetheless, it has been previously reported that comparable particle sizes, approximately <150 nm, can be achieved upon scaling up

mill sizes from the same manufacturer. Key parameters such as bead loading, agitator tip speed, stabilizer amount, and linear velocity of the slurry need to be analyzed during scaling up to achieve target particle sizes (Fisher 2006; Peltonen 2018).

One issue concerning the operation of this type of mill at high throughput rates is hydraulic packing. This phenomenon is related to the milling media being concentrated at the mill exit (packing), instead of remaining in the milling chamber during the operating cycle, which translates in reduced milling efficiency. Hydraulic packing can result in an increase in power consumption, together with an additional heat input to the sample batch (Fisher 2006). The flow rate that triggers hydraulic packing has been found to be related to increasing agitator tip speed, reduced bead loading, as well as the sample batch viscosity.

Another limitation found in milling processes performed in media mills is the potential for shedding of the media and components into the batch. It has been found that the use of glass beads yielded glass microparticles in the final product (Buchmann et al. 1996; Kipp 2004). Since no further purification steps are normally considered after milling of APIs, it is important during developmental stages of the process to assess the amount of objectionable substances in the batch. For API manufacture, these levels are normally in the parts per million range (Fisher 2006); however, they can be as high as 70 ppm, imposing development limitations in the process (Keck and Muller 2006). To overcome or limit the extent of these materials in the final batch, an additional premilling step that decreases the coarse particle size of the raw product can be performed to reduce the residence time of the batch in the wet mill, therefore reducing total shedding (Fisher 2006).

The wet-milling technology has been further developed by G. Liversidge and coworkers and turned into the high-energy media milling NanoCrystal technology by Elan for obtaining nanoscale nanocrystalline particle distributions of API (Liversidge et al. 1992). The nanoparticle dispersions obtained by this technology consist of the API and a surface stabilizer to avoid

aggregation and subsequent particle growth (Merisko-Liversidge and Liversidge 2008). To minimize the shedding of materials, the technology makes use of highly cross-linked polystyrene beads; however, the extent of erosion is dependent on a combination of the bead material and the physical characteristics of the drug (i.e., hardness) and the residence time (Keck and Muller 2006). The grinding process developed by Liversidge et al. has a limitation upon scaling up due to the heavy weight that it would impose, increasing the size of the mill.

While more research in the field is required to establish general guidelines in wet bead milling, some physical drug properties have been identified as key properties that determine malleability (Liu et al. 2019). Properties such as solid state (i.e., crystalline vs. amorphous) (Sharma et al. 2011), particle morphology (Liu et al. 2017, 2018a, b), particle size (Liu et al. 2018b), crystallite size (Liu et al. 2018b), and Young's modulus (Cerdeira et al. 2011) have all been found to be correlated with milling performance. More specifically, a porous particle morphology or a decrease in crystallite size prior to milling, obtained through spray drying of various drugs, has been associated with a further reduction in size after processing (Liu et al. 2018b).

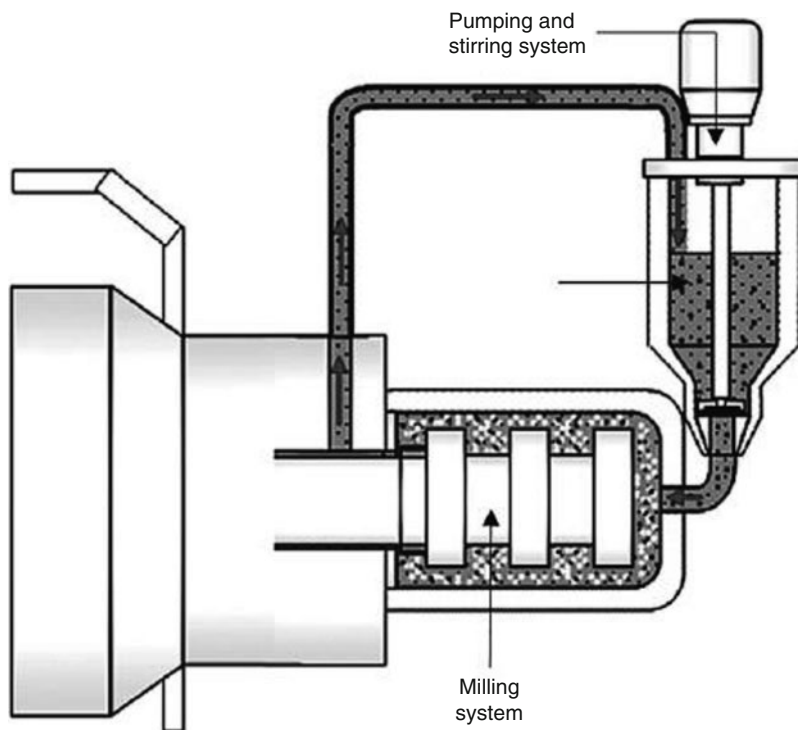
Particles obtained by media milling that are in the range of a few microns to the nanoscale are generally required to be stabilized using surface active agents or surfactants to prevent particle growth (Lee et al. 2005; Van Eerdenbrugh et al. 2008). The process normally begins with the formation of a macrosuspension in which the surfactant is added, followed by the wet-milling process itself. The surfactant to be used will be determined by a number of factors including the properties of the solid to be suspended (affinity of the solid with the surfactant), physical mechanism of action (electrostatic vs. steric stabilization), and route of administration of the nanosuspension (Berglund et al. 2003; Lee et al. 2005). Steric stabilization can be a more effective choice when there is a chance for poor gastrointestinal or systemic stability due to excess electrolytes. Ionic surfactants can also provide

sufficient stabilization by reducing the zeta potential, thus preventing particle aggregation. In many cases, the final choice is a combination of both steric and electrostatic stabilization using a combination of surfactants. There is a wide variety of surfactants that can be used for the development of nanosuspensions meant for oral administration; however, for the parenteral route, the choices are limited. Lecithins, Poloxamer 188, Tween 80, low-molecular weight polyvinylpyrrolidone (PVP), and sodium glycocholate (combined with lecithins) are surfactants that have been accepted for injection (Muller et al. 2006).

The number of different media mills available in the market range from laboratory-scale to industrial-scale volumes. Upon scaling up, there is need for equipment that can handle large volumes (and weights) of media and product. Since enlarging the whole milling unit would require a large amount of milling media, an external suspension container has been devised for operating mills with large-scale batches (Fig. 4.15). With this arrangement, an additional container feeds a suspension to the milling system in more discrete quantities, allowing a smaller mill to decrease the particle size of large quantities of feed. The downside of this strategy is the increase in milling times (Muller et al. 2006).

Generally, it may be understood that the use of a smaller bead size will yield a smaller resultant particle size. Li and colleagues demonstrated that decreasing bead sizes down to 50 μm resulted in a final nanosuspension mean size as low as 72 nm with polydispersity index values below 0.23 that had a relative short-term stability within the sub-100 nm mean size (Li et al. 2015). In another improvement upon bead properties, Funahashi and coworkers introduced the use of ice beads to produce a particle size reduction comparable to that observed with zirconia beads that led to similar rapid drug dissolution properties (Funahashi et al. 2019). The use of ice beads as a grinding media can lead to a contamination-free milling process due to the absence of shedding material.

Fig. 4.15 Bead mill DISP ERMAT (use register mark symbol) SL for mill base amounts of 50 mL 50 L. Schematic representation of the laboratory mill Dispermat SL. (Modified from Schilde et al. 2010)



Cryogenic Milling

The term cryomilling has been used in the literature to describe two different processes involving cryogenic conditions. The first is a grinding technique in which the solids are milled in a slurry formed with a cryogenic milling media. The other configuration consists of using a cryogenic liquid to decrease the temperature of the grinding chamber and mill the solids as in dry milling. Nonetheless, both operations rely on a cryogenic substance to control the temperature of the process while decreasing by attrition the average particle size (Witkin and Lavernia 2006). The direct and obvious advantage of the process is the suitability for thermally labile compounds; however, the removal of the cryogenic liquid upon finishing the milling process may impose certain limitations (Fisher 2006).

An investigation by Niwa et al. (2010) coined the term “ultra cryomilling” and was used for media milling that explicitly uses liquid nitrogen as dispersant (Fig. 4.16). Liquid nitrogen was used as the cryogenic liquid due to its poor solubilizing potency. Furthermore, the low

surface tension (8.85 mN/m at $-196\text{ }^{\circ}\text{C}$) and viscosity (0.158 mPa at $-196\text{ }^{\circ}\text{C}$) exhibited by liquid nitrogen might prevent secondary coaggregation and undesired particle growth. Additionally, materials under very low temperatures ($-196\text{ }^{\circ}\text{C}$ for liquid nitrogen) become more brittle and can be milled more efficiently (Reed 2007).

In the investigation by Niwa, after optimizing for size and amount of zirconia beads and agitation speed, crystalline nanoparticles were obtained (Niwa et al. 2010). The authors found that, by increasing the agitation speed of the shaft from 550 to 1600 rpm, the average particle size could be decreased. This was attributed to a higher kinetic energy imparted on the beads, thus creating high-impact collisions between particles and beads. The bead size in the 0.1–1 mm diameter range was found not to impact the performance of the milling process, both achieving similar particle-size distributions. For the purpose of comparing the performance of the novel cryomilling technique, the authors used 1 mm beads. Powders processed by the ultra

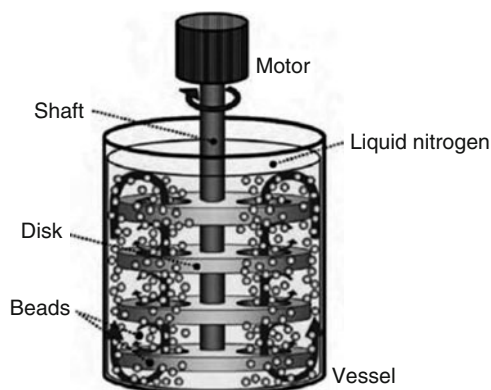


Fig. 4.16 Diagram of the ultra cryomilling apparatus in liquid nitrogen developed by Niwa et al. The beads, disks, shaft, and inner wall of the vessel were made of zirconia (Niwa et al. 2010)

cryomilling technique were comprised of 21.5% submicron particles, while powders processed by jet milling only achieved 9.07% of submicron particles (Niwa et al. 2010). The process was shown to work with a wide variety of drugs in terms of their physicochemical characteristics such as heat sensitivity and water solubility. It was further demonstrated that the crystalline structure found in the bulk solid remained after processing. One inherent limitation of the process though is the aggregation of particles upon liquid nitrogen evaporation. To account for this, the authors proposed an additional formulation design mainly focused on adding a surfactant to increase the wettability of the particles.

In recent years, this use of ultra cryomilling has seen progress in both the materials used and the processing technology (Sugimoto et al. 2012a, b). Phenytoin has been processed with ultra cryomilling to render much smaller particle sizes and more uniform in size in comparison with jet-milled drug, yet the dissolution rate was not improved due to aggregation. To overcome this limitation, Sugimoto et al. added a number of polymeric excipients (polyvinylpyrrolidone, Eudragit L100, hypromellose, hypromellose acetate-succinate, microcrystalline cellulose, hydroxypropylcellulose, and carboxymethyl cellulose) that provided stability to the nanosuspension and resulted in an improvement of the dissolution rate (Sugimoto et al. 2012b).

More recently, the ultra cryomilling process has been further modified by using dry ice as milling media. Not only were the particle sizes achieved comparable to that of the standard process, but also the authors found a yield increase due to the sublimation of both the milling liquid (liquid nitrogen) and media (dry ice as beads) (Sugimoto et al. 2012a).

4.4 High-Pressure Homogenization Techniques

Homogenization is a process by which the particle-size distribution of a suspension or an emulsion is narrowed or “homogenized,” thus decreasing the polydispersity of the sample. Particle breakage is achieved by a combination of high shear, turbulence, impact, as well as cavitation in the homogenizer. The type of homogenizer used determines which of these mechanisms will be more important for particle-size reduction together with the physical properties of the bulk powder.

4.4.1 Piston-Gap Homogenizers

Piston-gap homogenizers work with pure water as dispersant and rely on cavitation as the driving force for particle diminution. In these homogenizers, the suspension (or sometimes a coarse emulsion) passes through a very thin gap at very high velocities. Before entering the gap, the suspension is contained in a cylinder with a relatively large diameter compared to the width of the gap (Fig. 4.17). This tremendous decrease in diameter leads to an immense drop in the static pressure of the liquid. The resulting static pressure is below the vapor pressure of water, leading to boiling and the creation of gas bubbles that implode after leaving the gap, returning to normal pressure in the reservoir compartment of the homogenizer. This first technology, known as DissoCubes, considered this phenomenon, cavitation, as a primary factor in particle breakage (Muller et al. 1999).

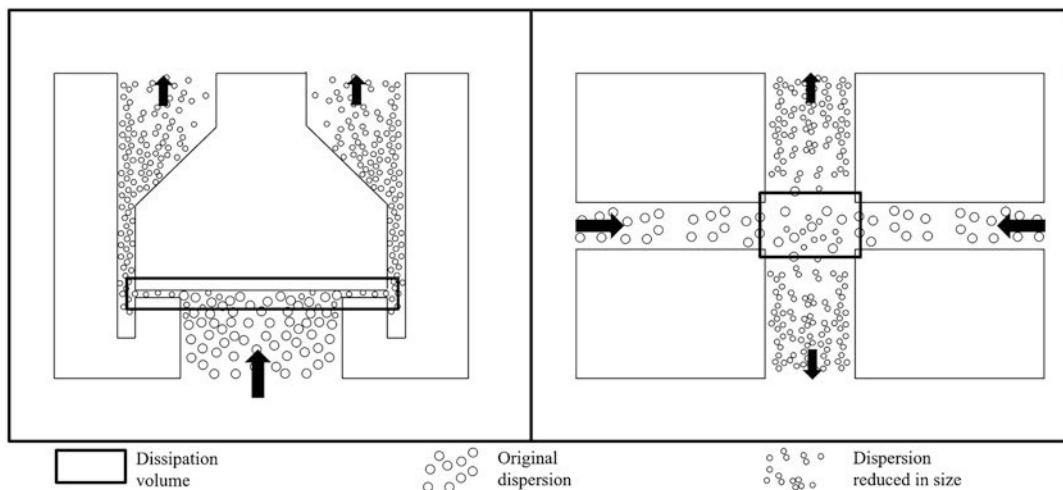


Fig. 4.17 Basic homogenization principles: piston-gap (left) and jet-stream arrangement (right). In the piston-gap homogenizer, the macrosuspension is forced to pass through a small gap (few microns), and particle breakage

is due to shear forces, cavitation, and impaction. In jet-stream homogenizers, the collision of two high-velocity streams leads to particle breakage mainly by impact forces. (Adapted from Muller et al. 2006)

Particle-size decrease is controlled by several factors: homogenization pressure, number of homogenization cycles, and hardness of the drug and stabilizers (Keck and Muller 2006). In general, increasing the pressure will translate to a decrease in average particle size; however, this relationship is not always linear. It has been found that up to a pressure of 4000 bar, there is a certain pressure above which particle-size diminution does not decrease any further (Fichera et al. 2004). The reason for this phenomenon appears to be that upon crystal breakage and particle-size reduction, the imperfections in particles become reduced in number per particle, thus decreasing the chance for particle breakage. A decrease in average particle size may also result from an increase in the number of homogenization cycles. In general, after five cycles, further increasing the number of cycles does not decrease the batch D_{50} (Keck and Muller 2006). Increasing the number of cycles to 15–20 does have an impact on the homogeneity of the sample and is reflected in a decrease of the batch D_{95} . As in other grinding techniques, softer material can be processed to achieve smaller average particle sizes when processing conditions are kept the same. Paclitaxel, a soft drug, has been reported in the 250 nm range after 10–20 homogenization cycles at 1500 bar. A harder drug, azodicarbonamide, has

been found to achieve particle sizes ranging from 500 to 800 nm, depending on the processing conditions (Keck and Muller 2006). Finally, the nature and concentration of the stabilizer (either surfactant or polymer) in the formulation, as opposed to emulsions, have been found to not affect the extent of particle-size diminution, although they do have an impact on aggregation in the long term (Muller et al. 1996).

4.4.2 Microfluidizer

The mechanism of particle-size reduction for this high-pressure homogenization technique is through the impaction of jet streams (Dearn 2000). As seen in Fig. 4.18, prehomogenized liquid is pumped through an interaction chamber where impaction occurs. The interaction chamber is composed of microchannels that split the liquid line in two. These two streams are then recombined at high velocities to produce forces of shear, impaction, and cavitation. These forces combine to cause particle breakage and size reduction. A detailed description of the operation and examples of the use of the microfluidizer can be found in US patent 4,553,254 (Cook and Lagace 1985).

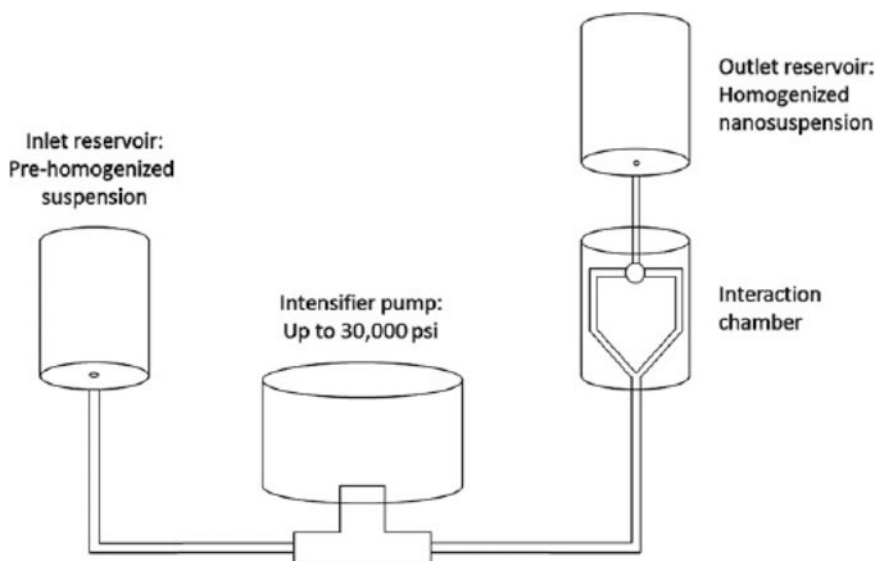


Fig. 4.18 Flow chart of the particle-size reduction process in the Microfluidizer. (Adapted from Singh and Naini 2006)

A disadvantage of this technology is that the product obtained can have a rather large quantity of particles in the larger size range (Illig et al. 1996). Furthermore, a high number of passes have been described in patents, reaching sometimes even 75 passes and ultimately translating into long processing times. Additionally, the system is more compatible with soft drugs, enabling nanosuspensions to be achieved during processing (Keck and Muller 2006; Muller et al. 2006). Larger particles often result when harder drugs are processed by this method, reducing the extent to which solubility can be increased through mechanical size reduction.

4.5 Combination of Top-Down and Bottom-Up in a Single Process for the Manufacture of Drug Nanosuspensions

Due to the limitations found in either wet ball milling or high-pressure homogenization such as the need of a micronized suspension as the starting material, and the long runtimes required for particle-size reduction, new strategies that combine top-down and bottom-up approaches have been recently described (Moeschwitzer and

Mueller 2006; Salazar et al. 2014). To this date, five combinative strategies have been described and are summarized in Table 4.6: NANOEDGE and nanoedge-like strategies, H 69, H 42, H 96, and CT.

4.5.1 NANOEDGE[®]

The NANOEDGE technology belongs to Baxter, and it was the first combinative technology described back in the early 2000s (Kipp et al. 2002, 2006). The technology combines a first step of microprecipitation based on antisolvent precipitation of the poorly water-soluble drug. For this, the drug is first dissolved in a water miscible organic solvent and then mixed with an aqueous solution that triggers the precipitation of poorly water-soluble drug. The resulting particles can either result in small size amorphous and/or semicrystalline particles suitable for the comminution step. This microprecipitation step is then followed by a high-pressure homogenization where particle size is further reduced and stabilized by either an enhancement of the crystallinity or by a rearrangement of the surface stabilizer (J.E. Kipp 2004). Although high-pressure homogenization is the conventional

Table 4.6 Combinative particle-size reduction techniques and the various drugs that have been used as examples

Combinative technology	Pretreatment	Size reduction technique	Drugs used	Smallest mean particle size achieved ^a	Administration route
NANOEDGE	Microprecipitation	High-pressure homogenization or sonication	Paclitaxel, nabumetone, prednisolone, carbamazepine, itraconazole	177 nm	Intravenous
Nanoedge-like	Microprecipitation	High-pressure homogenization or sonication	Meloxicam, isradipine, 10-hydroxycamptothecin, hydrocortisone, ibuprofen, nitrendipine, all-trans retinoic acid	80 nm	Oral
H 69	Cavi-precipitation	High-pressure homogenization	Ibuprofen, hydrocortisone acetate, resveratrol, omeprazole, prednisolone	22 nm	Oral
H 42	Spray-drying	High-pressure homogenization	Amphotericin B, glibenclamide, hydrocortisone acetate, ibuprofen, resveratrol	172 nm	Oral
H 96	Freeze-drying	High-pressure homogenization	Amphotericin B, glibenclamide, cyclosporine A, hydrocortisone acetate	62 nm	Oral
CT	Pearl milling	High-pressure homogenization	Rutin, hesperidin, apigenin	275 nm	Topical /oral

Full citation details can be found in Salazar et al. (2014)

^aIndicated as the smallest mean particle size of a specific studied drug. Each drug has its own particle-size reduction properties, including smallest particle size achieved

comminution step, other high-energy processes such as sonication or microfluidization can be used (Kipp et al. 2002, 2006). The remaining organic solvent from the antisolvent step represents a substantial limitation for product development, and particularly for the injectable development. The NANOEDGE technology and nanoedge-like technologies have been used to formulate a number of poorly water-soluble drugs (Table 4.6) including anticancer agents such as paclitaxel (Kipp 2004; Rabinow et al. 2004) and more recently quercetin (Qiao et al. 2020).

4.5.2 smartCrystal Technology

H 69 Technology

H 69 technology, along with H 42 and H96, is part of the smartCrystal technology family (Keck et al. 2008). Similar to the NANOEDGE

technology, H 69 involves antisolvent precipitation and high-pressure homogenization, yet the precipitation occurs in the presence of cavitation, hence cavi-precipitation (Table 4.6). The drug is dissolved in a suitable water-miscible organic solvent which is then incorporated into an aqueous solvent (nonsolvent of the drug) in the high-energy zone of a homogenizer. This results in particle formation, growth, and comminution occurring simultaneously as the high-pressure homogenization process advances through cavitation, particle collision, and shear forces (Müller and Möschwitzer 2015; Sinha et al. 2013). The high-energy homogenization process favors the crystallized state of nanoparticles, increasing their stability. The resulting nanosuspension also contains a portion of organic solvent which is a limitation requiring further processing toward the final product. At defined conditions, the H 69 technology can yield nanosuspensions as small as 22 and 27 nm with rather large

polydispersion (polydispersity indices 0.44–0.46) (Müller and Möschwitzer 2015).

H 42 Technology

Another application of the smartCrystal technology is termed H 42 and addresses the organic solvent issue found in technologies above. This method combines a particle manufacture step of spray drying followed by high-pressure homogenization (Salazar et al. 2013). The drug is first dissolved in an organic solvent and optionally mixed with surfactants or sugars to stabilize the solid during and after the spray drying step. In addition to the advantage of organic solvent removal, the resulting particles from the spray drying step are more breakable for the high-pressure homogenization step that follows (Moeschwitzer 2011). Another advantage of the H 42 technology is the reduction in the degree of crystallinity of the starting powders (spray dried), which results in the need for lower number of high-pressure homogenization cycles (reduction from 20 to 1 cycle) and positive particle-size performance (Liu et al. 2012; Salazar et al. 2014). The main limitation of this method of manufacture is associated to the heating required during the drying step, which could limit its use in thermolabile drugs (Moeschwitzer and Mueller 2006).

H 96 Technology

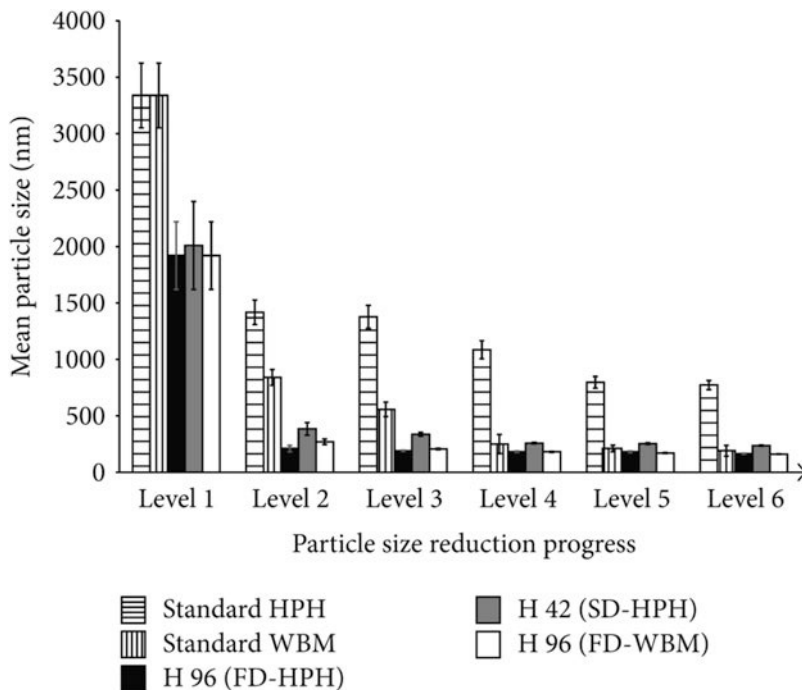
The last addition to the smartCrystal technology family is H 96 where the process begins with a freeze drying step followed by high-pressure homogenization (Moeschwitzer and Lemke 2008; Shegokar and Muller 2010). The process consists of dissolving the drug in an organic solvent that is then frozen with liquid nitrogen and subsequently freeze dried. Depending on the freeze drying conditions, the resulting material can present varying degrees of crystallinity and yet remain brittle for the latter high-pressure homogenization step (Salazar et al. 2011). Similar to the H 42 technology, in the H 69 technology, the organic solvent is removed prior to the high-pressure homogenization process, rendering the final

aqueous nanosuspension without further processing. The right choice of solvent or solvent mixtures to solubilize, freeze, and efficaciously lyophilization is key in the overall process performance and depends mainly on the drug (Salazar et al. 2012). As processing occurs at freezing temperatures, this technology enables particle-size reduction of thermolabile drugs. Although H 96 has been largely described for high-pressure homogenization as the secondary comminution process, studies have been conducted with wet-media (bead) milling demonstrating that the lyophilized brittle material can be processed into a nanosuspensions with both particle-size reduction strategies (Salazar et al. 2012). Figure 4.19 summarizes the particle-size reduction potential of the microprecipitation followed by high-pressure homogenization H 69, H 42, and H 96 technologies in comparison with conventional wet-media (bead) milling and high-pressure homogenization.

4.5.3 CT Technology

The Combination Technology (CT) is the only combination strategy that does not rely on the use of organic solvents and consists of two sequential top-down processes (Keck et al. 2008; Petersen 2015). This process consists of a low-energy pearl milling step followed by a high-pressure homogenization step. The first process reduces that size of a macrosuspension to a range between 600 and 1500 nm average size. The high-pressure homogenization stage further decreases particle size but more importantly provides the product with nanosuspension stability by bringing all larger particles to a homogeneous small particle size (decreasing the impact of Ostwald ripening) (Keck et al. 2008). Although this technology reaches average particle sizes larger than the aforementioned strategies, CT is advantageous due to the lower pressure required, shorter process length, and improved physical stability of nanosuspensions (Al Shaal et al. 2010).

Fig. 4.19 Particle-size reduction performance of standard and combinative technologies. Six levels of particle-size reduction progress are depicted: premilling (1), 1 High-pressure homogenization cycle at 1500 bar/1 hour of WBM (2), 5 cycles/2 hours (3), 10 cycles/4 hours (4), 15 cycles/8 hours (5), and 20 cycles/24 hours (6) (Salazar et al. 2014)



4.6 Conclusion

The number of new drugs and drug candidates with poor aqueous solubility is steadily increasing, and there is a need to address this solubility limitation. Decreasing the particle size of a substance achieves an increase in surface area by mass, can increase saturation solubility, and decreases diffusional distance, each of which ultimately results in an increase of either or both the extent and rate of dissolution for a given material. Top-down approaches that rely on mechanical particle-size reduction can be roughly classified into milling techniques and high-pressure homogenization techniques. Of these top-down strategies, wet-media milling, piston-gap homogenization, and microfluidization are the most popular. These widely used approaches may yield particle-size distributions in the low micron to the nanoscale range. Various technologies have been patented using such top-down approaches. Technologies such as NanoCrystal® by Elan and IDD-P® by SkyePharma are the only ones that yield particles in the nanoscale range and are currently used in marketed products. In addition to these successfully commercialized

technologies, there are several other methods in the pipeline that incorporate mechanical particle-size reduction using different techniques, demonstrating the growing acceptance of particle-size reduction as a means of improving the water solubility for a wide variety of existing and new active pharmaceutical ingredients.

Method Capsule 1: Particle-Size Reduction by Spiral Air Jet Milling

Based on the method reported by Schlocker et al. (2006).

Objective

- To obtain protein-loaded microparticles with adequate protein stability after processing. Horseradish peroxidase was used as model protein and was coprecipitated with either carbomer or a poly(methacrylate) prior to grinding.

Equipment and Materials

- Carbopol 934P and Eudragit L 100–55 as polymer matrix.
- Horseradish peroxidase as protein model.
- Spiral jet mill (Hosokawa Alpine Aeroplex 50 AS) with a diameter and height of grind-chamber 50 and 4.5 mm, respectively;

standard blowing-out nozzle; number of nozzles 4; nozzle diameter 0.8 mm; nozzle pitch 50°; and equipped with a temperature sensor (Lutron, DH-802C, Ming Chuan, Taiwan).

Method

- After coprecipitation of the model protein and one of the model polymer matrices, 1 g of the powder was added in the chamber of the spiral air jet mill.
- Injector air pressure was 7.5 bar.
- Grinding air pressure (GAP) was either 2.5 or 4.5 bar, and the powder was ground for 10 minutes.
- After milling, the material was collected from the grinding chamber and stored at -18 °C.

Results

- After laser diffraction analysis, it was revealed that increasing the GAP in the mill decreased the microparticles' size.
- Using isopropanol as the nonsolvent in the coprecipitation of the protein and carbomer and increasing the GAP from 2.5 to 4.5 bar decreased D50 from 5.2 to 2.7 μm. By using petroleum ether as the nonsolvent in the coprecipitation of the protein and poly (methacrylate) and increasing the GAP from 2.5 to 4.5, the D50 was decreased from 4.5 to 2.8 μm.
- A GAP of 4.5 bar in the case of the poly (methacrylate) reduced protein stability (measured as activity after processing) almost completely, while at 2.5 bar 58% activity remained. In the case of carbomer, increasing GAP from 2.5 to 4.5 bar decreased the remaining activity from 75 to 35%.
- The spiral air jet mill was found to be an effective process for the manufacture of protein-loaded microparticles with adequate protein stability after processing.

Method Capsule 2: Particle-Size Reduction by Media Milling

Based on the method reported by Liversidge et al. (1992).

Objective

- To obtain a suspension of PVP surface-modified crystalline danazol nanoparticles to improve bioavailability.

Equipment and Materials

- Wet-media mill with a 600 mL cylindrical vessel (inner diameter 7.6 cm).
- 200 mL of zirconia grinding media (0.85–1.18 mm diameter)
- Micronized danazol (mean particle size 10 μm).
- PVP K-15.

Method

- Zirconia grinding media was added to the vessel of the mill.
- Micronized danazol and PVP were added to the mill, and water was used as a dispersing agent to an adequate volume.
- The vessel was rotated horizontally around its axis at 57% of the critical speed.
- After 5 days of milling, the slurry was separated from the grinding media by sieving.

Results

- A sedimentation field flow fractionator was used for sizing and, after processing, the number average weight was 84.9 nm and the weight average weight was 169.1 nm.
- Particle size of the batch ranged from 26 to 340 nm.
- X-ray diffraction demonstrated that the crystalline structure of danazol remained unchanged after the process.
- Dispersions of unmilled danazol and the nanoparticulate slurry were dosed in beagles. The relative bioavailability of danazol from the nanoparticulate dispersion was 15.9-fold higher than from the danazol suspension containing microparticles (10 μm).

Method Capsule 3: Particle-Size Reduction by Ultra Cryomilling

Based on the method reported by Niwa et al. (2010).

Objective

- To obtain nanocrystals by a one-step milling process for drugs with a wide variety of

physical properties, such as heat sensitivity, oxidizability, or water solubility.

Equipment and Reagents

- Liquid nitrogen.
- Phenytoin.
- Batch-type wet mill with a 400-mL capacity vessel.
- Zirconia rotation shaft, disks, and beads.
- Sieve No. 60 (0.25 mm).

Method

- Similar to a typical wet-milling process, the drug is suspended in liquid nitrogen, and the suspension of drug and milling beads is vigorously agitated.
- Precool the parts of the mill (vessel, shaft, disks, and beads) with liquid nitrogen.
- Fill the milling vessel with 550 g of zirconia beads 1 mm diameter (approximately 150 mL).
- Suspend 15 g of phenytoin in liquid nitrogen and fill the milling chamber to 360 mL.
- Start and maintain a controlled agitation at 1600 rpm for 30 minutes, and pour additional liquid nitrogen to account for loss due to volatilization.
- Pass the slurry through a sieve to separate the powder from the beads.
- Collect the milled powder after all the liquid nitrogen evaporates.

Results

- After laser diffraction analysis, the particle-size profile revealed a D10, D50, and D90 of 0.62, 1.84, and 5.27 μm , respectively, with a 27.5% of submicron particles per batch.
- X-ray powder diffraction patterns and DSC curves indicated that the crystalline structure of particles before milling remained after the process.
- The crystalline habit of the particles remained the same as the initial.
- Milled particles tend to agglomerate; they may require a wetting agent for dispersion.

Method Capsule 4: Particle-Size Reduction by Piston-Gap High-Pressure Homogenization

Based on the method reported by Grau et al. (2000).

Objective

- To reproducibly obtain a 1% potency nanosuspension of 4-[N-(2-hydroxy-2-methyl-propyl)-ethanolamino]-2,7-bis(cis-2,6-dimethylmorpholin-4-yl)-6-phenyl-pteridine in water using a piston-gap high-pressure homogenizer.

Equipment and Materials

- Micron Lab 40 (APV Deutschland GmbH, Germany), 40 mL capacity high-pressure homogenizer.
- 4-[N-(2-hydroxy-2-methyl-propyl)-ethanolamino]-2,7-bis(cis-2,6-dimethylmorpholin-4-yl)-6-phenyl-pteridine
- Tween 80.
- Glycerol.

Method

- The drug is suspended in an aqueous solution containing the surfactants.
- At room temperature, the suspension is homogenized using a variable pressure profile.
- Two cycles are performed at 150 bar.
- Two more cycles are performed at 500 bar.
- Finally, 10 cycles are performed at 1500 bar.
- If needed, at the end of any cycle draw a slurry sample to determine particle size.
- At the end of the particle-size reduction process, collect the nanosuspension from the high-pressure homogenizer.

Results

- After the whole homogenization cycle (14 cycles), photon correlation spectroscopy revealed a mean diameter of 502 nm and a polydispersity index of 0.390.
- Laser diffraction data revealed D10, D50, and D90 of 0.31, 0.95, and 2.20 μm , respectively.
- High reproducibility was found for the mean size in between batches and at each cycle number with the parameters utilized in the high-pressure homogenization process.

Method Capsule 5: Particle-Size Reduction by Cavi-Precipitation Coupled with High-Pressure Homogenization

Based on the method reported by Sinha et al. (2013).

Objective

- To obtain ibuprofen nanocrystals by using the combined bottom-up and top-down approach of coupling cavi-precipitation with high-pressure homogenization.

Equipment and Materials

- Emulsiflex C5 (Avestin Europe GmbH, Mannheim, Germany) piston-gap homogenizer modified by inserting HPLC tubing to direct the antisolvent input as close as possible to the homogenization gap.
- Ibuprofen.
- Isopropanol.
- Hydroxypropyl methylcellulose (HPMCE5).
- Sodium dodecyl sulphate (SDS).

Method

- The drug (ibuprofen) is dissolved in the solvent phase (isopropanol).
- The antisolvent aqueous phase is composed of 0.1% w/v HPMCE5 and 0.2% w/v SDS.
- Set the homogenizer pressure to 1200–1300 bar and outside temperature to 0–1 °C through an iced water jacket.
- Set the antisolvent phase (aqueous) to 0–1 °C and incorporate into the high-pressure homogenizer.
- Incorporate all the solvent phase (organic solution containing ibuprofen) during the first homogenization cycle using an HPLC pump as close as possible to the homogenization gap.
- Continue the homogenization for 10 further cycles.

Results

- The optimum solvent/antisolvent ratio that yielded the smallest particle size (304 nm) was found to be 1.65/56.4.
- The ibuprofen concentration that resulted in the smallest particle size (304 nm) was 45.44 w/v.

- DSC and powder X-ray diffraction showed that crystallinity of ibuprofen remained after the precipitation and the high-pressure homogenization step as well.

Method Capsule 6: Particle-Size Reduction by Microprecipitation Followed by High-Pressure Homogenization

Based on the method reported by Qiao et al. (2020).

Objective

- To obtain quercetin nanocrystals by using the combined bottom-up and top-down approach of coupling microprecipitation with high-pressure homogenization.

Equipment and Materials

- NS1001L2K high-pressure homogenizer (Niro Soavi S.p.A. Co, Parma, Italy).
- Quercetin.
- mPEG-DCA,
- DMSO.

Method

- The drug (50 mg quercetin) is dissolved by sonication in the solvent (organic) phase (DMSO).
- The antisolvent aqueous phase is obtained by dissolving 25 mg of mPEG-DCA as stabilizer in 50 mL of distilled water.
- A presuspension is obtained by quickly adding the organic in the aqueous phase and stirring at 2000 rpm for 10 minutes at room temperature.
- The presuspension is then added to the high-pressure homogenizer and processed at various pressure and homogenization cycles to render a nanosuspension.
- The nanosuspension is then frozen and freeze dried to obtain a dry powder.

Results

- Large nanoparticles (332 nm) were achieved at 100 bar and 20 cycles; medium nanoparticles (159 nm) were achieved using 200–800 bars and 5–25 cycles; while small nanoparticles (30 nm) were achieved using a higher presuspension concentration of 250–1000 bars and 5–25 cycles.

- Quercetin nanoparticles exhibited enhanced antitumor efficacy and improved the immune response of treatment group.

Acknowledgments The authors thank the support from FONDECYT Regular Project 1181689, ANID/PIA/ACT192144, and FONDAP Project 15130011, all granted by Chilean National Agency for Research and Development (ANID).

References

- Afolabi A, Akinlabi O, Bilgili E. Impact of process parameters on the breakage kinetics of poorly water-soluble drugs during wet stirred media milling: a microhydrodynamic view. *Eur J Pharm Sci.* 2014;51:75–86. <https://doi.org/10.1016/j.ejps.2013.09.002>.
- Agrawal S, Ashokraj Y, Bharatam PV, Pillai O, Panchagnula R. Solid-state characterization of rifampicin samples and its biopharmaceutical relevance. *Eur J Pharm Sci.* 2004;22(2–3):127–44. <https://doi.org/10.1016/j.ejps.2004.02.011>.
- Al Shaal L, Müller RH, Shegokar R. smartCrystal combination technology--scale up from lab to pilot scale and long term stability. *Pharmazie.* 2010;65(12):877–84.
- Albus FE. The modern fluid energy mill. *Chem Eng Prog.* 1964;60(6):102–6.
- am Ende D, Rose P. Strategies to achieve particle size of active pharmaceutical ingredients. In: Abdel-Magid A, Caron S, editors. *Fundamentals of early clinical drug development: from synthesis design to formulation.* Hoboken: Wiley-Interscience; 2006. p. 247–67.
- Ambrus R, Gieszinger P, Gáspár R, Sztójkov-Ivanov A, Ducza E, Márki Á, Janáky T, Tömösi F, Kecskeméti G, Szabó-Révész P, Bartos C. Investigation of the absorption of nanosized lamotrigine containing nasal powder via the nasal cavity. *Molecules.* 2020;25(5):1065. <https://doi.org/10.3390/molecules25051065>.
- Atiemo-Obeng V, Calabrese R. Rotor-stator mixing devices. In: Paul E, Atiemo-Obeng V, Kresta S, editors. *Handbook of industrial mixing: science and practice.* Hoboken: Wiley-Interscience; 2004. p. 479–505.
- Bell TA. Challenges in the scale-up of particulate processes—an industrial perspective. *Powder Tech.* 2005;150(2):60–71. <https://doi.org/10.1016/j.powtec.2004.11.023>.
- Bentham AC, Kwan CC, Boerefijn R, Ghadiri M. Fluidised-bed jet milling of pharmaceutical powders. *Powder Tech.* 2004;141(3):233–8. <https://doi.org/10.1016/j.powtec.2004.01.024>.
- Berglund K, Przybycien T, Tilton R. Coadsorption of sodium dodecyl sulfate with hydrophobically modified nonionic cellulose polymers. 1. Role of polymer hydrophobic modification. *Langmuir.* 2003;19(7):2705–13. <https://doi.org/10.1021/la026429g>.
- Bilgili E, Afolabi A. A combined microhydrodynamics–polymer adsorption analysis for elucidation of the roles of stabilizers in wet stirred media milling. *Int J Pharm.* 2012;439(1–2), 193–206. <https://doi.org/10.1016/j.ijpharm.2012.09.040>.
- Bisrat M, Nyström C. Physicochemical aspects of drug release VIII. The relation between particle size and surface specific dissolution rate in agitated suspensions. *Int J Pharm.* 1988;47(1–3):223–31. [https://doi.org/10.1016/0378-5173\(88\)90235-9](https://doi.org/10.1016/0378-5173(88)90235-9).
- Bitterlich A, Laabs C, Busmann E, Grandeur A, Juhnke M, Bunjes H, Kwade A. Challenges in nanogrinding of active pharmaceutical ingredients. *Chem Eng Technol.* 2014;37(5):840–6. <https://doi.org/10.1002/ceat.201300697>.
- Blecher L, Schwedes J. Energy distribution and particle trajectories in a grinding chamber of a stirred ball mill. *Int J Miner Process.* 1996;44–45:617–27. [https://doi.org/10.1016/0301-7516\(95\)00070-4](https://doi.org/10.1016/0301-7516(95)00070-4).
- Blecher L, Kwade A, Schwedes J. Motion and stress intensity of grinding beads in a stirred media mill. Part 1: energy density distribution and motion of single grinding beads. *Powder Tech.* 1996;86(1):59–68. [https://doi.org/10.1016/0032-5910\(95\)03038-7](https://doi.org/10.1016/0032-5910(95)03038-7).
- Böhm BHL, Grau MJ, Hildebrand GE, Thünnemann AF, Müller RH. Preparation and physical properties of nanosuspensions (DissoCubes™) of poorly soluble drugs. *Proc Intern Symp Control Rel Bioact Mater.* 1998;25:956–7.
- Boundy M, Leith D, Polton T. Method to evaluate the dustiness of pharmaceutical powders. *Ann Occup Hyg.* 2006;50(5):453–8. <https://doi.org/10.1093/annhyg/mel004>.
- Bruno J, Doty B, Gustow E, Illig K, Rajagopalan N, Sarpotdar P. Method of grinding pharmaceutical substances. 1996. Retrieved from <http://www.google.com/patents/about?id=qLQaAAAAEBAJ&dq=5,518,187>. Accessed 21 May 1996.
- Buchmann S, Fischli W, Thiel F, Alex. Aqueous microsuspension, an alternative intravenous formulation for animal studies. In 42nd Annual Congress of the International Association for Pharmaceutical Technology (APV), Mainz; 1996. p. 124.
- Cordeira AM, Gander B, Mazzotti M. Role of milling parameters and particle stabilization on nanogrinding of drug substances of similar mechanical properties. *Chem Eng Technol.* 2011;34(9):1427–38.
- Chamayou A, Dodds JA. Air jet milling. In: Williams JC, Allen T, editors. *Handbook of powder technology*, vol. 12. Amsterdam: Elsevier; 2007. p. 421–35.
- Chan HK, Doelker E. Polymorphic transformation of some drugs under compression. *Drug Dev Ind Pharm.* 1985;11(2–3):315–32. <https://doi.org/10.3109/03639048509056874>.
- Chaumeil J. Micronization: a method of improving the bioavailability of poorly soluble drugs. *Methods Find Exp Clin Pharmacol.* 1998;20(3):211–6.
- Chikhaliya V, Forbes R, Storey R, Ticehurst M. The effect of crystal morphology and mill type on milling induced

- crystal disorder. *Eur J Pharm Sci.* 2006;27(1):19–26. <https://doi.org/10.1016/j.ejps.2005.08.013>.
- Chow AHL, Tong HHY, Chattopadhyay P, Shekunov BY. Particle engineering for pulmonary drug delivery. *Pharm Res.* 2007;24(3):411–37. <https://doi.org/10.1007/s11095-006-9174-3>.
- Clark AR, Shire SJ. Formulation of proteins for pulmonary drug delivery. In: McNally EJ, editor. *Protein formulation and delivery*. New York: M. Dekker; 2000. p. 201–34.
- Clement S, Purutyan H. Narrowing down equipment choices for particle-size reduction. *Chem Eng Prog.* 2002;98(6):50.
- Colombo I, Grassi G, Grassi M. Drug mechanochemical activation. *J Pharm Sci.* 2009;98(11):3961–86.
- Cook EJ, Lagace AP. Apparatus for forming emulsions. 1985. Retrieved from <http://www.google.com/patents/about?id=H6gtAAAEB AJ&dq=apparatus+for+forming+emulsions>. Accessed 6 Aug 1985.
- de Vegt O, Vromans H, den Toonder J, van der Voort MK. Influence of flaws and crystal properties on particle fracture in a jet mill. *Powder Tech.* 2009;191(1–2):72–7. <https://doi.org/10.1016/j.powtec.2008.09.014>.
- de Villiers M. Influence of cohesive properties of micronized drug powders on particle size analysis. *J Pharm Biomed Anal.* 1995;13(3):191–8. [https://doi.org/10.1016/0731-7085\(95\)01274-O](https://doi.org/10.1016/0731-7085(95)01274-O).
- de Villiers M, Tiedt L. An analysis of fine grinding and aggregation of poorly soluble drug powders in a vibrating ball mill. *Pharmazie.* 1996;51(8):564–7.
- Dearn AR. Atovaquone pharmaceutical compositions. 2000, January 25. Retrieved from <http://www.google.com/patents/about?id=2iEDAAAEB AJ&dq=Atovaquone+pharmaceutical+compositions>. Accessed 25 Jan 2000.
- Dong Y, Feng S. Poly(D, L-lactide-co-glycolide) (PLGA) nanoparticles prepared by high pressure homogenization for paclitaxel chemotherapy. *Int J Pharm.* 2007;342(1–2):208–14. <https://doi.org/10.1016/j.ijpharm.2007.04.031>.
- Eckhoff R. Dust explosion hazards in the ferro-alloys industry. In: 52nd electric furnace conference. 1994, pp 283–302.
- Eckhoff R. Dust explosions – origin, propagation, prevention, and mitigation: an overview. In: Eckhoff R, editor. *Dust explosions in the process industries*. 3rd ed. New York: Gulf Professional; 2003. p. 1–156.
- Eckhoff R. Current status and expected future trends in dust explosion research. *J Loss Prev Process Indust.* 2005;18(4–6):225–37. <https://doi.org/10.1016/j.jlp.2005.06.012>.
- Elan Drug Technologies – Commercialized Products. Retrieved December 9, 2010, from http://www.elandrugtechnologies.com/nanocrystal_technology/commercialised. Accessed 9 Dec 2010.
- Eskin D, Zhupanska O, Hamey R, Moudgil B, Scarlett B. Microhydrodynamic analysis of nanogrinding in stirred media mills. *AIChE J.* 2005a;51(5):1346–58. <https://doi.org/10.1002/aic.10392>.
- Eskin D, Zhupanska O, Hamey R, Moudgil B, Scarlett B. Microhydrodynamics of stirred media milling. *Powder Technol.* 2005b;156(2–3):95–102. <https://doi.org/10.1016/j.powtec.2005.04.004>.
- Fichera M, Wissing S, Müller R. Effect of 4000 bar homogenisation pressure on particle diminution in drug suspensions. (2004. pp 679–680..
- Fisher E. Milling of active pharmaceutical ingredients. In: Swarbrick J, editor. *Encyclopedia of pharmaceutical technology*. 3rd ed. New York: Informa Healthcare; 2006. p. 2339–51.
- Fontana F, Figueiredo P, Zhang P, Hirvonen JT, Liu D, Santos HA. Production of pure drug nanocrystals and nano co-crystals by confinement methods. *Adv Drug Deliv Rev.* 2018;131:3–21. <https://doi.org/10.1016/j.addr.2018.05.002>.
- Friedrich A. Size reduction overview: shear, compression, and impact. *Powder Bulk Eng.* 2001;15(6):19–25.
- Funahashi I, Kondo K, Ito Y, Yamada M, Niwa T. Novel contamination-free wet milling technique using ice beads for poorly water-soluble compounds. *Int J Pharm.* 2019;563:413–25. <https://doi.org/10.1016/j.ijpharm.2019.04.008>.
- Gieszinger P, Tomuta I, Casian T, Bartos C, Szabó-Révész P, Ambrus R. Definition and validation of the design space for co-milled nasal powder containing nanosized lamotrigine. *Drug Dev Ind Pharm.* 2018;44(10):1622–30.
- Godet-Morand L, Chamayou A, Dodds JA. Talc grinding in an opposed air jet mill: start-up, product quality and production rate optimization. *Powder Technol.* 2002;128(2–3):306–13. [https://doi.org/10.1016/S0032-5910\(02\)00172-9](https://doi.org/10.1016/S0032-5910(02)00172-9).
- Grau MJ, Kayser O, Muller RH. Nanosuspensions of poorly soluble drugs: reproducibility of small scale production. *Int J Pharm.* 2000;196(2):155–9. [https://doi.org/10.1016/S0378-5173\(99\)00411-1](https://doi.org/10.1016/S0378-5173(99)00411-1).
- Gribbon P, Andreas S. High-throughput drug discovery: what can we expect from HTS? *Drug Discov Today.* 2005;10(1):17–22. [https://doi.org/10.1016/S1359-6446\(04\)03275-1](https://doi.org/10.1016/S1359-6446(04)03275-1).
- Hamelmann F, Schmidt E. Methods of estimating the dustiness of industrial powders—a review. *Kona.* 2003;21:7–18.
- Hancock BC, Parks M. What is the true solubility advantage for amorphous pharmaceuticals? *Pharm Res.* 2000;17(4):397–404.
- Hassan S, Lau R. Effect of particle formulation on dry powder inhalation efficiency. *Curr Pharm Des.* 2010;16(21):2377–87.
- Hoyer H, Schlocker W, Krum K, Bernkop-Schnürch A. Preparation and evaluation of microparticles from thiolated polymers via air jet milling. *Eur J Pharm Biopharm.* 2008;69(2):476–85. <https://doi.org/10.1016/j.ejpb.2008.01.009>.
- Illig K, Mueller R, Ostrander K, Swanson J. Use of microfluidizer processing for preparation of pharmaceutical suspensions. *Pharmaceut Tech.* 1996;20(10):78–88.

- Ito H. Scale-up theory of single track jet mill. In: Proceedings of the 2nd Korea-Japan powder technology symposium, vol 63. 1987.
- Jacobs C, Kayser O, Müller RH. Nanosuspensions as a new approach for the formulation of the poorly soluble drug tarazepide. *Int J Pharm.* 2000;196(2):161–4. [https://doi.org/10.1016/S0378-5173\(99\)00412-3](https://doi.org/10.1016/S0378-5173(99)00412-3).
- Kaiser F, Nied R. Modern jet pulverizers. *Aufbereitungs Technik.* 1980;10:507–14.
- Kalepu S, Nekkanti V. Insoluble drug delivery strategies: review of recent advances and business prospects. *Acta Pharm Sin B.* 2015;5(5):442–53.
- Keck C, Muller R. Drug nanocrystals of poorly soluble drugs produced by high pressure homogenisation. *Eur J Pharm Biopharm.* 2006;62(1):3–16. <https://doi.org/10.1016/j.ejpb.2005.05.009>.
- Keck CM, Kobierski S, Mauludin R, Müller RH. Second generation of drug nanocrystals for delivery of poorly soluble drugs: smartCrystals technology. *Dosis.* 2008;24(2):124–8.
- Kesisoglou F, Panmai S, Wu Y. Nanosizing – oral formulation development and biopharmaceutical evaluation. *Adv Drug Deliv Rev.* 2007;59(7):631–44. <https://doi.org/10.1016/j.addr.2007.05.003>.
- Kipp J. The role of solid nanoparticle technology in the parenteral delivery of poorly water-soluble drugs. *Int J Pharm.* 2004;284(1–2):109–22. <https://doi.org/10.1016/j.ijpharm.2004.07.019>.
- Kipp J, Wong JT, Doty M, Rebbeck C.. Microprecipitation method for preparing submicron suspensions. 2002, November 28. Retrieved from <http://www.google.com/patents/US20020176935>
- Kipp JE, Wong JCT, Doty MJ, Rebbeck CL. Microprecipitation method for preparing submicron suspensions. (2006, May 2. Retrieved from <http://www.google.com/patents/US7037528>
- Koivisto M, Heinänen P, Tanninen VP, Lehto V. Depth profiling of compression-induced disorders and polymorphic transition on tablet surfaces with grazing incidence x-ray diffraction. *Pharm Res.* 2006;23(4): 813–20. <https://doi.org/10.1007/s11095-006-9785-8>.
- Kwade A. Wet comminution in stirred media mills – research and its practical application. *Powder Technol.* 1999;105(1–3):14–20. [https://doi.org/10.1016/S0032-5910\(99\)00113-8](https://doi.org/10.1016/S0032-5910(99)00113-8).
- Kwade A. A stressing model for the description and optimization of grinding processes. *Chem Eng Tech.* 2003;26(2):199–205. <https://doi.org/10.1002/ceat.200390029>.
- Kwade A, Schwedes J. Breaking characteristics of different materials and their effect on stress intensity and stress number in stirred media mills. *Powder Technol.* 2002;122(2):109–21.
- Kwade A, Schwedes J. Wet grinding in stirred media mills. In: Salman A, Ghadirri M, Hounslow M, editors. *Handbook of powder technology*, vol 12, Particle breakage. Amsterdam: Elsevier; 2007. p. 251–382.
- Lee I, Variankaval N, Lindemann C, Starbuck C. Rotor-stator milling of APIs-empirical scale-up parameters and theoretical relationships between the morphology and breakage of crystals. *Am Pharmaceut Rev.* 2004;7: 120–3.
- Lee J, Lee S, Choi J, Yoo J, Ahn C. Amphiphilic amino acid copolymers as stabilizers for the preparation of nanocrystal dispersion. *Eur J Pharm Sci.* 2005;24(5): 441–9. <https://doi.org/10.1016/j.ejps.2004.12.010>.
- Li M, Yaragudi N, Afolabi A, Dave R, Bilgili E. Sub-100 nm drug particle suspensions prepared via wet milling with low bead contamination through novel process intensification. *Chem Eng Sci.* 2015;130:207–20. <https://doi.org/10.1016/j.ces.2015.03.020>.
- Lipinski CA. Drug-like properties and the causes of poor solubility and poor permeability. *J Pharmacol Toxicol Methods.* 2000;44(1):235–49. [https://doi.org/10.1016/S1056-8719\(00\)00107-6](https://doi.org/10.1016/S1056-8719(00)00107-6).
- Lipinski CA, Lombardo F, Dominy BW, Feeney PJ. Experimental and computational approaches to estimate solubility and permeability in drug discovery and development settings. *Adv Drug Deliv Rev.* 1997;23(1–3):3–25. [https://doi.org/10.1016/S0169-409X\(96\)00423-1](https://doi.org/10.1016/S0169-409X(96)00423-1).
- Liu T, Müller RH, Möschwitzer JP. Process optimization of a novel particle size reduction technology H 42. *Tag Der Pharmazie, (Abstract P33)*, 25. 2012.
- Liu T, Müller RH, Möschwitzer JP. Systematical investigation of a combinative particle size reduction technology for production of resveratrol nanosuspensions. *AAPS PharmSciTech.* 2017;18(5):1683–91.
- Liu T, Müller RH, Möschwitzer JP. Production of drug nanosuspensions: effect of drug physical properties on nanosizing efficiency. *Drug Dev Ind Pharm.* 2018a;44 (2):233–42.
- Liu T, Müller RH, Möschwitzer JP. Consideration of the solid state for resveratrol nanocrystal production. *Powder Technol.* 2018b;332:63–9. <https://doi.org/10.1016/j.powtec.2018.03.028>.
- Liu T, Yu X, Yin H, Möschwitzer JP. Advanced modification of drug nanocrystals by using novel fabrication and downstream approaches for tailor-made drug delivery. *Drug Deliv.* 2019;26(1):1092–103. <https://doi.org/10.1080/10717544.2019.1682721>.
- Liversidge E, Wei L. Stabilization of chemical compounds using nanoparticulate formulations. 2003. Retrieved from <http://www.google.com/patents/about?id=IjyGAAAAEBAJ>. Accessed 20 Mar 2003.
- Liversidge G, Cundy K, Bishop J, Czekai D Surface modified drug nanoparticles. 1992. Retrieved from <http://www.google.com/patents/about?id=48caAAAAEBAJ&dq=5,145,684>. Accessed 8 Sep 1992.
- Merisko-Liversidge E, Liversidge G. Drug nanoparticles: formulating poorly water-soluble compounds. *Toxicol Pathol.* 2008;36(1):43–8. <https://doi.org/10.1177/0192623307310946>.
- Merisko-Liversidge E, Sarpotdar P, Bruno J, Hajj S, Wei L, Peltier N, Rake J, et al. Formulation and antitumor activity evaluation of nanocrystalline

- suspensions of poorly soluble anticancer drugs. *Pharm Res.* 1996;13(2):272–8.
- Merisko-Liversidge E, Liversidge G, Cooper E. Nanosizing: a formulation approach for poorly-water-soluble compounds. *Eur J Pharm Sci.* 2003;18(2):113–20. [https://doi.org/10.1016/S0928-0987\(02\)00251-8](https://doi.org/10.1016/S0928-0987(02)00251-8).
- Midoux N, Hosek P, Pailleres L, Authelin J. Micronization of pharmaceutical substances in a spiral jet mill. *Powder Tech.* 1999;104(2):113–20. [https://doi.org/10.1016/S0032-5910\(99\)00052-2](https://doi.org/10.1016/S0032-5910(99)00052-2).
- Moschwitz J. Method for producing ultrafine submicronic suspensions. 2011, October 11. Retrieved from <http://www.google.com/patents/US8034381>
- Moschwitz J, Lemke A. Method for the gentle production of ultrafine particle suspensions and ultrafine particles and the use thereof. 2008, August 14. Retrieved from <http://www.google.com/patents/US20080193520>
- Moschwitz J, Mueller RH. New method for the effective production of ultrafine drug nanocrystals. *J Nanosci Nanotechnol.* 2006;6(9–10):3145–53. <https://doi.org/10.1166/jnn.2006.480>.
- Muller, R. H., & Moschwitz, J. (2015, October 27). Method and device for producing very fine particles and coating such particles. Retrieved from <http://www.google.com/patents/US9168498>
- Muller F, Polke R. From the product and process requirements to the milling facility. *Powder Tech.* 1999;105(1–3):2–13. [https://doi.org/10.1016/S0032-5910\(99\)00112-6](https://doi.org/10.1016/S0032-5910(99)00112-6).
- Muller R, Peters K, Becker R, Kruss B. Nanosuspensions – a novel formulation for the iv administration of poorly soluble drugs. In: 1st World Meeting APGI/APV, pp 491–492, Budapest. 1995.
- Muller R, Peters K, Craig D. Electron microscopic studies of nanosuspensions – particle shapes as a funktion of drug and surfactant. In: 23rd international symposium of controlled release of bioactive materials. Japan: Kyoto; 1996. p. 925–6.
- Muller R, Becker R, Kruss B, Peters K. Pharmaceutical nanosuspensions for medicament administration as systems with. 1999. Retrieved from <http://www.google.com/patents/about?id=TIoXAAAEBAJ&dq=5,858,410>. Accessed 12 Jan 1999.
- Muller RH, Jacobs C, Kayser O. Nanosuspensions as particulate drug formulations in therapy: rationale for development and what we can expect for the future. *Adv Drug Deliv Rev.* 2001;47(1):3–19. [https://doi.org/10.1016/S0169-409X\(00\)00118-6](https://doi.org/10.1016/S0169-409X(00)00118-6).
- Muller R, Jacobs C, Kayser O. DissoCubes: a novel formulation for poorly soluble and poorly bioavailable drugs. In: Rathbone M, Hadgraft J, Roberts M, editors. *Modified-release drug delivery technology*. 1st ed. New York: Marcel Dekker; 2003. p. 135–49.
- Muller R, Moschwitz J, Bushrab F. Manufacturing of nanoparticles by milling and homogenization techniques. In: Gupta R, Kompella U, editors. *Nanoparticle technology for drug delivery*. New York: Taylor & Francis; 2006. p. 21–51.
- Murdande SB, Pikal MJ, Shanker RM, Bogner RH. Solubility advantage of amorphous pharmaceuticals: I. a thermodynamic analysis. *J Pharm Sci.* 2010;99:1254–64. <https://doi.org/10.1002/jps.21903>.
- Nakach M, Authelin J, Chamayou A, Dodds J. Comparison of various milling technologies for grinding pharmaceutical powders. *Miner Engg.* 2004;74(Suppl 1):S173–81. <https://doi.org/10.1016/j.minpro.2004.07.039>.
- New Food Pharma Systems Spiral Jet Mill: Introduction. 2010. Retrieved December 16, 2010, from <http://www.labx.com/v2/adsearch/detail3.cfm?adnumb=406756>
- Nied R. Rotor impact mills. In: Salman A, Ghadiri M, Hounslow M, editors. *Handbook of powder technology, Particle breakage*, vol. 12. Amsterdam: Elsevier; 2007. p. 229–49.
- Niwa T, Nakanishi Y, Danjo K. One-step preparation of pharmaceutical nanocrystals using ultra cryo-milling technique in liquid nitrogen. *Eur J Pharm Sci.* 2010;41(1):78–85. <https://doi.org/10.1016/j.ejps.2010.05.019>.
- Noyes AA, Whitney WR. The rate of solution of solid substances in their own solutions. *J Am Chem Soc.* 1897;19(12):930–4. <https://doi.org/10.1021/ja02086a003>.
- Peltonen L. Design space and QbD approach for production of drug nanocrystals by wet media milling techniques. *Pharmaceutics.* 2018;10(3):104.
- Peltonen L, Hirvonen J. Pharmaceutical nanocrystals by nanomilling: critical process parameters, particle fracturing and stabilization methods. *J Pharm Pharmacol.* 2010;62(11):1569–79. <https://doi.org/10.1111/j.2042-7158.2010.01022.x>.
- Petersen R. Nanocrystals for use in topical cosmetic formulations and method of production thereof. 2015, August 25. Retrieved from <http://www.google.com/patents/US9114077>
- Qiao Y, Cao Y, Yu K, Zong L, Pu X. Preparation and antitumor evaluation of quercetin nanosuspensions with synergistic efficacy and regulating immunity. *Int J Pharm.* 2020;589:119830. <https://doi.org/10.1016/j.ijpharm.2020.119830>.
- Rabinow B. Nanosuspensions in drug delivery. *Nat Rev Drug Discov.* 2004;3(9):785–96. <https://doi.org/10.1038/nrd1494>.
- Rabinow BE, Gupta P, Wong J, Papadopoulos P, Chaubal M. Formulation of water-insoluble antineoplastic agents as nanosuspensions using NANOEDGE formulation technology. *Cancer Res.* 2004;64(7 Suppl):146.
- Rasenack N, Müller B. Micron-size drug particles: common and novel micronization techniques. *Pharm Dev Technol.* 2004;9(1):1–13. <https://doi.org/10.1081/PDT-120027417>.
- Reed R. Trends and advances in cryogenic materials. In: Timmerhaus K, Reed R, editors. *Cryogenic*

- engineering: fifty years of progress. Dordrecht: Springer; 2007. p. 52–83.
- Rohrs BR, Amidon GE, Meury RH, Seccrest PJ, King HM, Skoug CJ. Particle size limits to meet USP content uniformity criteria for tablets and capsules. *J Pharm Sci.* 2006;95(5):1049–59. <https://doi.org/10.1002/jps.20587>.
- Salazar J, Heinzerling O, Müller RH, Möschwitzer JP. Process optimization of a novel production method for nanosuspensions using design of experiments (DoE). *Int J Pharm.* 2011;420(2):395–403. <https://doi.org/10.1016/j.ijpharm.2011.09.003>.
- Salazar J, Ghanem A, Müller RH, Möschwitzer JP. Nanocrystals: comparison of the size reduction effectiveness of a novel combinative method with conventional top-down approaches. *Eur J Pharm Biopharm.* 2012;81(1):82–90. <https://doi.org/10.1016/j.ejpb.2011.12.015>.
- Salazar J, Müller RH, Möschwitzer JP. Performance comparison of two novel combinative particle-size-reduction technologies. *J Pharm Sci.* 2013;102(5):1636–49. <https://doi.org/10.1002/jps.23475>.
- Salazar J, Müller RH, Möschwitzer JP. Combinative particle size reduction technologies for the production of drug nanocrystals. *J Pharmaceut.* 2014, Article ID 265754.
- Schilde C, Nolte H, Arlt C, Kwade A. Effect of fluid-particle-interactions on dispersing nano-particles in epoxy resins using stirred-media-mills and three-roll-mills. *Compos Sci Technol.* 2010;70(4):657–63. <https://doi.org/10.1016/j.compscitech.2009.12.021>.
- Schlocker W, Gschließer S, Bernkop-Schnürch A. Evaluation of the potential of air jet milling of solid protein-poly(acrylate) complexes for microparticle preparation. *Eur J Pharm Biopharm.* 2006;62(3):260–6. <https://doi.org/10.1016/j.ejpb.2005.09.001>.
- Schurr GA, Zhao QQ. Fluid mechanic considerations for fine grinding in a fluid energy mill., 1994, p. 536.
- Schwenzfeuer K, Glor M, Gitzi A. Relation between ignition energy and limiting oxygen concentration for powders. 2001. p. 909.
- Sharma P, Denny W, Garg S. Effect of wet milling process on the solid state of indomethacin and simvastatin. *Int J Pharm.* 2009;380(1–2):40–8. <https://doi.org/10.1016/j.ijpharm.2009.06.029>.
- Sharma P, Zujovic ZD, Bowmaker GA, Denny WA, Garg S. Evaluation of a crystalline nanosuspension: polymorphism, process induced transformation and in vivo studies. *Int J Pharm.* 2011;408(1):138–51. <https://doi.org/10.1016/j.ijpharm.2011.01.032>.
- Shegokar R, Müller RH. Nanocrystals: industrially feasible multifunctional formulation technology for poorly soluble actives. *Int J Pharm.* 2010;399(1–2):129–39. <https://doi.org/10.1016/j.ijpharm.2010.07.044>.
- Shoyele S, Cawthorne S. Particle engineering techniques for inhaled biopharmaceuticals. *Adv Drug Deliv Rev.* 2006;58(9–10):1009–29. <https://doi.org/10.1016/j.addr.2006.07.010>.
- Simonelli AP, Mehta SC, Higuchi WI. Inhibition of sulfathiazole crystal growth by polyvinylpyrrolidone. *J Pharm Sci.* 1970;59(5):633–8. <https://doi.org/10.1002/jps.2600590512>.
- Singh S, Naini V. Homogenization and homogenizers. In: Swarbrick J, editor. *Encyclopedia of pharmaceutical technology.* 3rd ed. New York: Informa Healthcare; 2006. p. 1996–2003.
- Sinha B, Müller RH, Möschwitzer JP. Systematic investigation of the cavi-precipitation process for the production of ibuprofen nanocrystals. *Int J Pharm.* 2013;458(2):315–23. <https://doi.org/10.1016/j.ijpharm.2013.10.025>.
- Skelton R, Khayyat A, Temple R. Fluid energy milling—an investigation of micronizer performance. *Fine particles processing.* 1980;1:113–25.
- SkyePharma—Insoluble Drug Delivery Platform. Retrieved December 9, 2010., from http://www.skyepharma.com/Technology/Oral_Technology/Particle_Engineering_Technologies/Insoluble_Drug_Delivery_Platform/Default.aspx?id=80. Accessed 9 Dec 2010.
- Smit W. Jetmilling of heat sensitive materials, world congr part technol, part II. Nurnberg: Comminution; 1986.
- Spencer R, Dalder B. Sizing up grinding mills. *Chem Eng.* 1997;104(4):84–7.
- Stairmand CJ. The energy efficiency of milling processes: a review of some fundamental investigations and their application to mill design. Vol. 1975;79:1–17.
- Steckel H, Markefka P, teWierik H, Kammelar R. Effect of milling and sieving on functionality of dry powder inhalation products. *Int J Pharm.* 2006;309(1–2):51–9. <https://doi.org/10.1016/j.ijpharm.2005.10.043>.
- Stein J, Fuchs T, Mattern C. Advanced milling and containment technologies for superfine active pharmaceutical ingredients. *Chem Eng Tech.* 2010;33(9):1464–70. <https://doi.org/10.1002/ceat.200900590>.
- Stenger F, Mende S, Schwedes J, Peukert W. Nanomilling in stirred media mills. *Chem Eng Sci.* 2005;60(16):4557–65. <https://doi.org/10.1016/j.ces.2005.02.057>.
- Stevenson B. Preventing disaster: analyzing your plant's dust explosion risks. *Powder Bulk Eng.* 2001;15(1):19–27.
- Sugimoto S, Niwa T, Nakanishi Y, Danjo K. Development of a novel ultra cryo-milling technique for a poorly water-soluble drug using dry ice beads and liquid nitrogen. *Int J Pharm.* 2012a;426(1–2):162–9. <https://doi.org/10.1016/j.ijpharm.2012.01.007>.
- Sugimoto S, Niwa T, Nakanishi Y, Danjo K. Novel ultra-cryo milling and co-grinding technique in liquid nitrogen to produce dissolution-enhanced nanoparticles for poorly water-soluble drugs. *Chem Pharm Bull.* 2012b;60(3):325–33. <https://doi.org/10.1248/cpb.60.325>.
- Tangsathitkulchai C. Effects of slurry concentration and powder filling on the net mill power of a laboratory ball mill. *Powder Tech.* 2003;137(3):131–8. <https://doi.org/10.1016/j.powtec.2003.08.048>.
- Trasi NS, Boerrigter SXM, Byrn SR. Investigation of the milling-induced thermal behavior of crystalline and

- amorphous griseofulvin. *Pharm Res.* 2010;27(7):1377–89. <https://doi.org/10.1007/s11095-010-0129-3>.
- Troester F. Cremophor-free aqueous paclitaxel nanosuspension production and chemical stability. 2004.
- Van Eerdenbrugh B, Van den Mooter G, Augustijns P. Top-down production of drug nanocrystals: Nanosuspension stabilization, miniaturization and transformation into solid products. *Int J Pharm.* 2008;364(1):64–75. <https://doi.org/10.1016/j.ijpharm.2008.07.023>.
- Ward GH, Schultz RK. Process-induced crystallinity changes in albuterol sulfate and its effect on powder physical stability. *Pharm Res.* 1995;12(5):773–9.
- Wilén C, Moilanen A, Rautalin A, Torrent J, Conde E, Lodel R, Carson D, et al. Safe handling of renewable fuels and fuel mixtures. Technical Research Centre of Finland (VTT); 1999.
- Witkin D, Lavernia E. Synthesis and mechanical behavior of nanostructured materials via cryomilling. *Prog Mater Sci.* 2006;51(1):1–60. <https://doi.org/10.1016/j.pmatsci.2005.04.004>.
- Zhang GGZ, Law D, Schmitt EA, Qiu Y. Phase transformation considerations during process development and manufacture of solid oral dosage forms. *Adv Drug Deliv Rev.* 2004;56(3):371–90. <https://doi.org/10.1016/j.addr.2003.10.009>.